Protein attenuation as a mechanism of robustness to gene duplication in protein complexes

Diana Ascencio[1,2,3,4,5,6], Guillaume Diss[1,2,3,5,7], Isabelle Gagnon-Arsenault[1,2,3,4,5], Alexandre K Dubé[1,2,3,4,5], Alexander DeLuna[6], Christian R. Landry[1,2,3,4,5]

1. Regroupement québécois de recherche sur la fonction, l'ingénierie et les applications des protéines (PROTEO), Québec QC, Canada, G1V 0A6,
2. Institut de Biologie Intégrative et des Systèmes (IBIS), Université Laval, Québec QC, Canada, G1V 0A6,
3. Centre de Recherche en Données Massives de l'Université Laval, Université Laval, Québec QC, Canada, G1V 0A6,
4. Département de biochimie, de microbiologie et de bio-informatique, Université Laval, Québec QC, Canada, G1V 0A6,
5. Département de biologie, Université Laval, Québec QC, Canada, G1V 0A6,
6. Unidad de Genómica Avanzada (Langebio), Centro de Investigación y de Estudios Avanzados, 36824 Irapuato, GTO, México
7. Current affiliation: Friedrich Miescher Institute for Biomedical Research, Basel, Switzerland.

Corresponding Author:
Christian Landry (christian.landry@bio.ulaval.ca)
Room 3106, Pavillon Charles-Eugène-Marchand
1030, Avenue de la Médecine
Université Laval
Québec (Québec) G1V 0A6
Canada
Téléphone: 418-656-3954

Keywords: Gene duplication; Gene balance hypothesis; Protein attenuation; Posttranslational regulation; Copy number variation; Protein-protein interactions; Protein complexes

Abstract

Gene duplication is ubiquitous and is a major driver of phenotypic diversity across the tree of life, but its immediate consequences are not fully understood. Immediate deleterious effects would diminish the probability of retention of duplicates and thus prevent their contribution to long term evolution. One deleterious effect of duplication could be the perturbation of the stoichiometry of protein complexes. We measured the fitness effects of the duplication of 900 essential genes in the budding yeast using high-resolution competition assays. At least ten percent of genes caused a fitness disadvantage when duplicated. Intriguingly, the duplication of most protein complex subunits had small to non-detectable effects on fitness, with few exceptions. We selected four complexes with subunits that had an impact on fitness when duplicated and measured the impact of individual gene duplications on their protein-protein interactions. We found that very few duplications affect both fitness and interactions. Furthermore, we found that large complexes such as the 26S proteasome are protected from gene duplication by posttranslational attenuation of protein abundance. The presence of regulatory mechanisms that maintain the stoichiometric balance of protein complexes may therefore protect from the dosage effects of gene duplication. Our results show that a better understanding of protein regulation and assembly in complexes is required for the refinement of current models of gene duplication.

Significance statement:

Many studies have focused on the mechanisms of long-term retention of gene duplicates such as the gain of functions or their reciprocal losses. However, such changes are more likely to occur if the duplicates are maintained for a long period. This time span will be short if duplication is immediately deleterious. We measured the distribution of fitness effects of gene duplication for 900 genes in budding yeast. We find that gene duplication is more likely to be deleterious than beneficial. However, and contrary to previous models, gene duplication generally does not affect fitness by altering the organization of protein complexes. We show that post-translational attenuation may protect complexes from the effects of gene duplication.

Introduction

Gene duplication and divergence is a primary source of functional innovation and diversity. Some genes are often retained in duplicates in genomes, while others are more likely to be found as single-copy. During the last few decades, the long term maintenance of gene duplicates through the gain or reciprocal loss of function (respectively, neo or subfunctionalization) has been studied extensively (Ohno, 1970; Lynch & Force, 2000; Qian & Zhang, 2008). However, we know relatively little about the immediate impact of duplications, which may have significant consequences on the preservation of paralogs. Genes with adverse effects on fitness upon duplication would have a reduced residence time in populations, thereby limiting their contribution to long term evolution. For instance, even modest changes in gene dosage such as those caused by duplication sometimes produce significant phenotypic effects, both positive and negative (Iskow et al., 2012; Qian & Zhang, 2014; Rice & McLysaght, 2017a). This is commonly referred to as dosage-sensitivity. Understanding the immediate impact of duplication is, therefore, of paramount importance.

Several mechanisms have been suggested to explain dosage-sensitivity. These include concentration dependency, promiscuous off-target interactions at high concentration, and dosage imbalance (Rice & McLysaght, 2017b). The gene balance hypothesis predicts that the single-gene duplication of protein complex subunits is harmful, as this can lead to an immediate stoichiometric imbalance with the rest of the subunits (Birchler & Veitia, 2007; Rice & McLysaght, 2017b). There are indirect pieces of evidence that support such prediction: complex subunits are less likely to be retained after small-scale duplication, are often co-expressed at similar levels, and are enriched among genes that reduce fitness when underexpressed (Gonçalves et al., 2017; Papp et al., 2003). For instance, haploinsufficiency, defined as a dominant phenotype in diploid organisms that are heterozygous for a loss-of-function allele, is more common among genes that encode protein complex subunits (Deutschbauer et al., 2005). However, other works have shown that genes that are toxic when overexpressed are not enriched as part of protein complexes (Semple et al., 2008; Sopko et al., 2006). This suggests that overexpression can be deleterious for reasons unrelated to complex stoichiometry.

While gene deletion and overexpression experiments inform us of how cells respond to lowered or increased abundance of proteins, they are fundamentally different from a naturally occurring duplication. For instance, the use of non-native promoters and multicopy plasmids may cause the assayed genes to be overexpressed several-fold and may also alter the timing of expression. In addition, if dosage-fitness relationships are non-linear, results from overexpression cannot be interpolated to gene duplication. For these reasons, and because fitness rather than complex assembly has been assayed in previous experiments (Moriya et al., 2012; Sopko et al., 2006), we do not know what is the impact of duplication on the assembly of protein complexes.

One reason why the overexpression of protein complex subunits can be less detrimental than a reduction of expression is dosage regulation (Semple et al., 2008). The correct dosage of protein subunits appears to be tightly regulated by the cell. For instance, members of multiprotein complexes are produced in precise proportion to their stoichiometry in both bacteria (Li et al., 2014) and eukaryotes (Taggart & Li, 2018). In *Saccharomyces cerevisiae*, proportional synthesis is sometimes maintained by tuning the protein synthesis rates for duplicated genes that encode the same subunit (Taggart & Li, 2018). Additionally, recent studies revealed that the abundance of members of multiprotein complexes is often attenuated or buffered in aneuploids (strains with extra copies of one or several chromosomes) (Chen et al., 2019; Dephoure et al., 2014; Gonçalves et al., 2017). A study by Dephoure *et. al* (2014) suggested that attenuation may be quite common since nearly 20% of the proteome is attenuated in aneuploids. They discovered

that most attenuated genes (60-76%) are members of multiprotein complexes (Dephoure et al., 2014). In fact, (Chen et al., 2019) found that up to 50% of subunits with imbalanced gene copy numbers (compared with the rest of the complex) may be attenuated to normal protein abundance levels. Since attenuated genes have mRNA transcript levels and protein synthesis rates proportional to their gene-copy number, the regulation of attenuated genes is likely to occur posttranslationally (Dephoure et al., 2014; Ishikawa et al., 2017; Taggart & Li, 2018). However, aneuploid cells may not be the best models to study the effect of small-scale gene duplications because a large proportion of their genome is duplicated at once. In addition, aneuploid cells often experience systemic effects like proteotoxic stress (Oromendia et al., 2012), which may cause pleiotropic consequences on protein synthesis and degradation rates that are challenging to disentangle from those of the duplication of a single gene. Furthermore, when a complete chromosome is duplicated, more than one subunit -- or the complete set of subunits of a complex -- may be duplicated, which could lessen or even prevent the effects of stoichiometric imbalance. Therefore, the extent and the nature of attenuation after small duplication events are yet to be explored systematically.

In this work, we sought to measure the immediate impact of gene duplication by experimentally simulating gene duplication of essential genes in yeast. We focused on this set because genes that are essential for growth are enriched in protein complexes (Papp et al., 2003). Genes that are essential are also less likely to be duplicated, which means that additional copies in the genome will not confound the results of duplication. We measured the fitness consequences of individual gene duplication for nearly 900 genes in individual strain competitions. We measured changes in protein-protein interactions (PPIs) in response to gene duplication for a subset of essential genes that are part of four large protein complexes. We also measured the extent to which the expression of proteasome subunits is attenuated as a response to gene duplication. Our results show that even though gene duplication often affects fitness, it has a small effect on the assembly of protein complexes. Finally, we show that the apparent robustness of multi-protein complexes to gene duplication is likely to be a consequence of posttranslational attenuation.

Results

An important percentage of yeast's essential genes affect fitness when duplicated

We measured the fitness effects of gene duplication at high-resolution using competition assays with fluorescently labeled cells in co-culture (Figure 1A). We individually duplicated 899 essential genes using single-copy centromeric plasmids expressing the genes under their native promoters and UTRs (Ho et al., 2009). In parallel, we generated a distribution of control strains in which we competed a *WT* strain (also used as a reference) with itself. Each of the 192 replicates of this control set is an independent colony from a transformation.

We found that for most genes (86%), duplication has little or no effect on relative fitness (-0.01> $s < 0.01$, $-4.5 >$ *z-score* < 4.5). However, around 9% (Figure 1B) of the duplications have moderate to strong deleterious effects ($s < -0.01$, z-score < -4.5) while 4% have beneficial ($s > 0.01$, z-score > 4.5) but often modest effects. We validated the top 180 genes (top 180 absolute z-scores) using the same growth conditions but monitoring the two populations by flow cytometry. For this purpose, we generated the strain constructions *de novo* and tested three biological replicates per sample. While less scalable, this approach allows for a more accurate estimation of population ratios, since fluorescence is measured at the single-cell level instead of the population level. There is a strong correlation between the two assays (Pearson's $r = 0.83$, $p < 10e\text{-}15$, Figure 1C), giving us good confidence in the accuracy of our large-scale measurements. We validated the vast majority of the effects of the first competition assay (159/180, Figure 1C). Since the impact of duplication may be dependent on the environmental condition, as is the case for aneuploidies (Pavelka et al., 2010), we performed a parallel competition experiment on a condition of ionic and osmotic stress (1.2M NaCl). We find a significant correlation between conditions (Pearson's correlation $r = 0.67$, $p < 10e\text{-}15$), and a similar number of deleterious (8.5%) and beneficial (4.6%) effects (*Supplementary Figure S2*). Many of the effects may, therefore, be general but some are condition specific.

Around four percent of the duplications have beneficial effects above 1% (z-score > 4.5) (Figure 1B). Among the genes with beneficial effects, we find metabolic regulatory genes such as *CDC25* and *IRA1* (Figure 1B-C), which regulate the Ras-cAMP pathway (Broek et al., 1987; Russell et al., 1993; Tanaka et al., 1989). In yeasts, growth, and metabolism in response to nutrients, particularly glucose, are regulated to a large degree by this pathway. Since we used glucose as a carbon source, duplication of these two genes may modify the activity of the pathway in a way that increases the growth rate. The duplication of some genes that encode central metabolism enzymes were also beneficial. For instance, duplication of *HIP1*, a histidine transporter (Tanaka & Fink, 1985) and *PDC2*, a pyruvate decarboxylase (Schmitt & Zimmermann, 1982; Velmurugan et al., 1997) may result in increased growth rate through metabolic activity in a similar manner to duplication of genes in the Ras-cAMP pathway.

Deleterious duplications are more frequent, have stronger effects, and include genes that were previously reported to be toxic upon overexpression such as *TUB1*, *TUB2,* and *ACT1*. The products of these genes are involved in the structural integrity of the cell cytoskeleton and have been previously shown to be highly sensitive to dosage increase (Burke et al., 1989; Espinet et al., 1995; Katz et al., 1990). Here, we show that adding a single copy of the gene on a centromeric plasmid is enough to cause a strong fitness defect. Our results also support recent observations that doubling or halving the expression of TUB1 and TUB2 reduces fitness (Keren et al., 2016). Consistent with these results, we find that 19% of haploinsufficient genes, as defined by Deutschbauer *et al*. (2005), produce deleterious effects when duplicated (17/88, Figure 1D). This is more than two times the percentage of haplosufficient genes (8%) (61/811; *Pearson's* χ^2 *test* $p < 1e\text{-}3$; Figure 1D). Conversely, this trend is not significant for haploinsufficient genes that lead to increased fitness when duplicated (6/88 and 34/811; *Pearson's* χ^2 *test* $p = 0.388$; Figure 1D).

Hence, at least 19% of haploinsufficient genes are also sensitive to increased dosage, revealing that the fitness effects of gene doubling are not particularly well predicted by the effect of reduction in gene dosage.

The gene balance hypothesis predicts that both under- and over-expression of a protein complex's subunit would cause deleterious phenotypes since dosage perturbation affects the stoichiometric balance between the subunits of the complex and compromises its assembly (Birchler & Veitia, 2007). Haploinsufficient genes are enriched among essential genes and are also more likely to code for protein complex subunits (Deutschbauer et al., 2005). For instance, some subunits of the RNA polymerase II (Rpb2p) and of the proteasome (Rpn3p) are both haploinsufficient and deleterious when duplicated. This indicates that such proteins are sensitive to changes in gene-dosage in both directions, just as the gene balance hypothesis predicts. However, when we mapped the fitness effects of gene duplication on annotated yeast protein complexes, we find no significant difference compared to genes that are not in complexes (*Wilcoxon rank-sum test p = 0.28;* Figure 1E). In fact, both gene categories share a similar percentage of deleterious effects (8% and 9%, respectively). It is important to notice that all of these findings are robust to different z-score thresholds (*Supplementary Table S3*). Therefore, the duplication of members of protein complexes is not generally associated with a decrease in fitness, in apparent contradiction with the gene balance hypothesis.

Figure 1

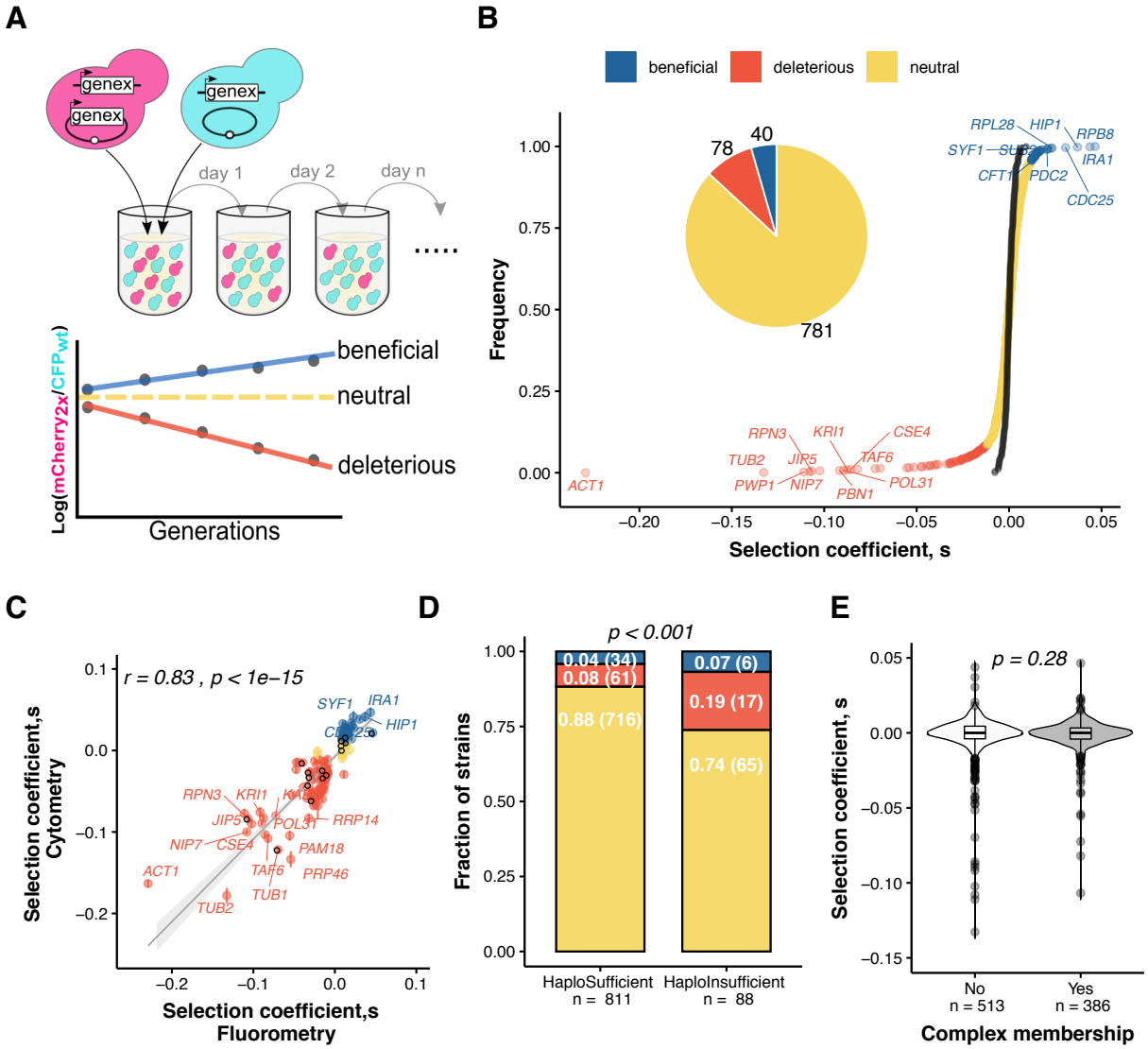

Figure 1. **More than 10% of yeast essential genes affect fitness when duplicated.** (**A**) Relative fitness was measured using a high-resolution competition assay (DeLuna et al., 2008). We co-cultured a mCherry-tagged strain carrying an extra-copy of an essential gene on a centromeric plasmid with a CFP-tagged reference strain carrying a control plasmid. We followed the ratio of the two populations for up to 28 generations to calculate a slope, which corresponds to the selection coefficient (*s*). (**B**) Cumulative distribution of selection coefficients of all the 899 strains tested (*Supplementary Table S1)*. Each colored dot represents a strain expressing an additional gene copy. The black dots represent the distribution of 192 biological replicates of reference versus reference competition. The threshold used for deleterious (in red) or beneficial (in blue) effect is at least 1% (-4.5 < z score > 4.5). (**C**) Selection coefficients for the validation of the 180 top hits measured by flow cytometry (*Supplementary Table S2)*. The gene labels are for genes with the strongest deleterious and beneficial effects. The bars indicate the standard deviation of three biological replicates. The black circles highlight genes with HaploInsufficient phenotypes. Pearson's

correlation coefficient results are indicated on top. (**D**) A comparison of fitness effects among HaploInsufficient and HaploSufficient genes (Deutschbauer et al., 2005). We show Fisher's exact-test results on top. The fraction and number of genes are indicated with white letters. (**E**) Comparison of the selection coefficients of proteins that are members of complexes and proteins that are not. On top, we show the p-value of a Wilcoxon's Rank-Sum test.

The duplication of individual subunits rarely affects PPIs in complexes

Our results so far indicate that the predicted deleterious fitness effects potentially due to gene-dosage imbalance is only present in some complexes. However, it is not clear if these effects are a consequence of their subunit PPI perturbations. With this question in mind and based on our fitness screening, we selected complexes that are sensitive to gene-dosage changes (the 26S proteasome and the three RNA polymerases) to investigate the effects of gene duplication on their PPI network *in vivo*. We measured pairwise PPIs between all pairs of subunits before and after the duplication of each subunit, using a Protein-fragment Complementation Assay (PCA) based on the DHFR enzyme (DHFR-PCA). The quantitative nature of PCA allows us to estimate a perturbation score (*ps*) as a direct measure of the effects of gene duplication on the PPI network of a complex (Figure 2A).

We first used the strategy on the retromer, a small, well-characterized, and non-essential complex, which has been reported to have PPIs sensitive to gene deletion (Diss et al., 2013). Retromer genes were not included in the fitness assays but we used this complex to show the principle of the experiments. This complex is associated with endosomes and is required for endosome-to-Golgi retrieval of receptors (e.g. the Vps10 protein) that mediate delivery of hydrolases to the yeast vacuole (Mukadam & Seaman, 2015). Functionally, the retromer is divided into two subcomplexes: a cargo-selective trimer of Vps35p, Vps29p, and Vps26p and a membrane-bending dimer of Vps5p and Vps17p (Seaman et al., 1998). DHFR-PCA detects significant interactions from all the retromer subunits (*Supplementary Figure S5A*). From our PCA data, we detect same-subunit competition effects between fused and non-fused copies of the proteins. Since the extra copy of the duplicated subunit is not tagged with a DHFR reporter fragment, it titrates PPI partners away from the tagged copy, resulting in a decreased colony size for all the interactions of this subunit (Figure 2A). For instance, we see a reduction of the interaction of all Vps5p PPIs upon duplication of *VPS5* (Figure 2A). We also find that the duplication increases the strength of the interactions between Vps35p-Vps26p, members of the other subcomplex, the cargo-selective trimer (Figure 2A). These results show that our strategy has enough resolution to detect small perturbations in the PPIs after the duplication of a single gene coding for a complex subunit.

We next examined the effect of gene duplication on four complexes with proteins whose gene duplication alters fitness, as identified in our previous analysis, namely the proteasome and the RNA polymerases. The proteasome is a highly conserved and thoroughly described eukaryotic protein complex which is amenable to study by DHFR-PCA (Chrétien et al., 2018; Tarassov et al., 2008). In yeast, the core complex (20S) is associated with the regulatory particle (19S) to form a large complex (26S) composed of 37 subunits (Fischer et al., 1994; Hochstrasser et al., 1999). From hereinafter, we will refer to the 26S proteasome as just proteasome. We tested pairwise interactions among 21 subunits as baits and 16 subunits as preys that belong to either the regulatory particle or the core complex. We detected 47 PPIs between subunits in the *WT* strain (*Supplementary Figure S5B*). The three RNA polymerases are also well-described large complexes: RNApol I includes 14 subunits, RNApol II has 16, and RNApol III has 18 subunits (Archambault & Friesen, 1993; Cramer, 2002; Sentenac, 1985). We tested all combinations between all available subunits since five subunits are shared between the three RNA

polymerases. We observed 33 significant PPIs out of 689 combinations tested between 31 baits and 26 preys in a *WT* background (*Supplemental Figure S5C*).

We observed that most subunit duplications have small to non-detectable effects on the interaction network of their complex and are weakly correlated with a fitness effect. We first examined same-subunit competition effects (Figure 2B, *Wilcoxon's rank-sum test p < 10e-15*), which validates that additional copies of the proteins are expressed and that we can measure quantitative changes in their PPIs. Indeed, 135/181 cases show a reduced interaction score. In the case of the proteasome, excluding competition cases, only 46 out of 8917 combinations tested were significantly different (FDR-corrected *q-value < 0.05*) from the *WT* interactions within the complex; while for the three RNA polymerases, only 28 out of 21341 combinations tested were significantly different (Figure 2C). Overall, most of the significant perturbations are gains of PPIs (55/74), which may suggest that when a duplication alters the interaction dynamics within the complex it does so by increasing the strength or amount of PPIs of other subunits (Figure 2C-D). The strongest effects are seen for the duplication of *PRE7*, especially in two interactions Pup1p-Pre5p and Pre8p-Rpn8p (indicated in Figure 2D). Pup1p, Pre5p, and Pre8p are part of the same subcomplex that includes Pre7p and they interact closely during the formation of the 20S proteasome. Pup1p is the β2 subunit while Pre5p and Pre8p are the α6 and α2 subunits, respectively (Budenholzer et al., 2017). Additionally, these subunits share close spatial proximity, ranging from 66 to 178 Å (Chrétien et al., 2018). To explore the possible correlation between PPIs and fitness effects, we calculated the mean *ps* for each subunit (mean of the absolute values of significant perturbation-scores) and compared it with the selection coefficient of strains containing a gene-duplication of the same subunit (Figure 2E). The correlation between *ps* and fitness is significant (*Pearson's r = -0.47, p = 0.031*), but this correlation is driven mainly by Pre7p from the 20S proteasome. These results suggest that subunit duplications typically have little or no effect on the protein interaction network within the complex, at least for the tested complexes.

Figure 2

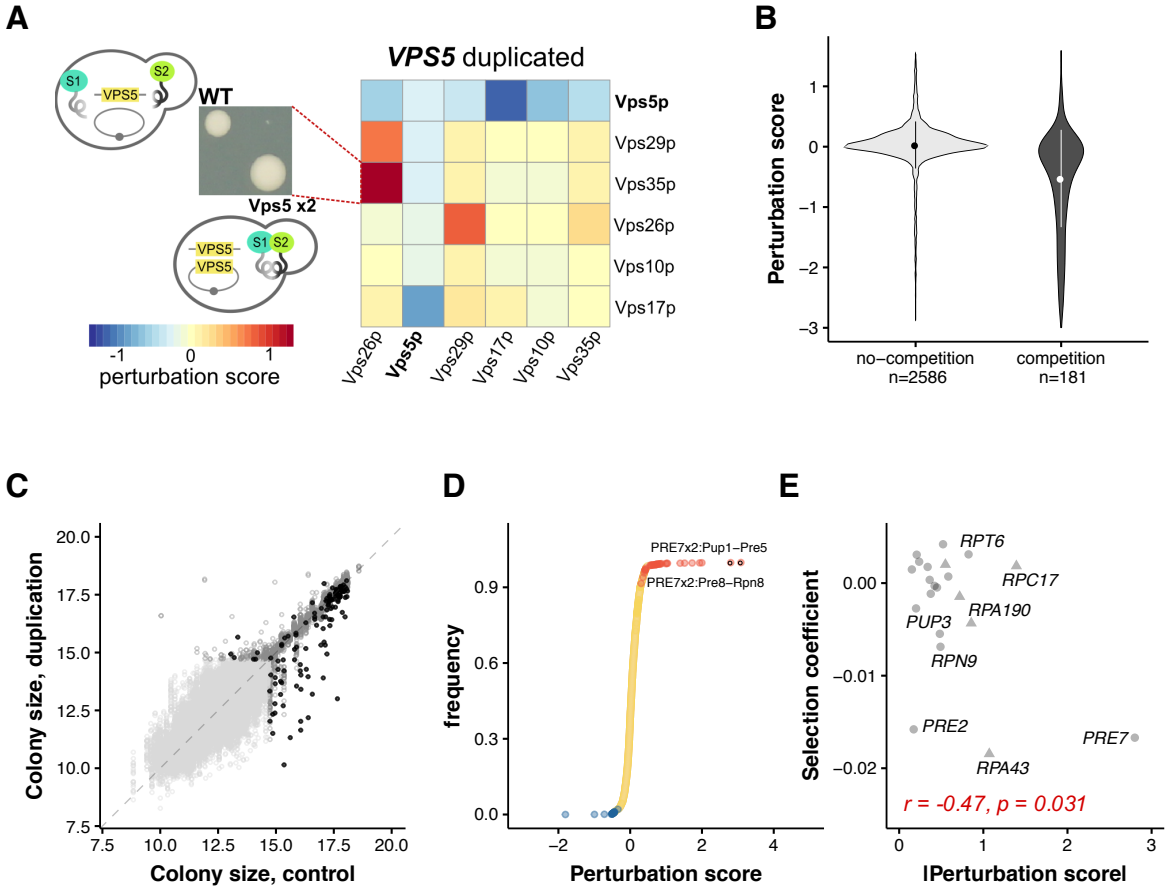

Figure 2. Most duplications of subunits do not affect PPIs in large complexes. (**A**) DHFR PCA-based strategy to measure perturbation of the pairwise physical interactions after a duplication. On the left, in a DHFR-PCA the colony size on selective media (MTX) is proportional to the stability and strength of the physical interaction between the two subunits (shown in green). The perturbation-score (*ps*) is defined as the colony size difference between the strain carrying a duplication (+pCEN-*VPS5*) and a *WT* (+pCEN) strain. We show a heatmap indicating *ps* values of the complete retromer PPI network due to the duplication of *VPS5*. (**B**) Distributions of *ps* for interactions with and without a competing subunit. Since the duplicated protein is not tagged with a DHFR fragment, it titrates PPI partners away from the tagged copy, decreasing colony size. We show violin plots of the distributions of all the interactions tested for five complexes (*Supplementary Table S5*). (**C**) Colony sizes of all strains carrying the duplication of a subunit compared with their control strain (the empty vector). Colony sizes of diploid strains carrying all tested combinations of preys, baits, and duplications for proteasome, and the three RNA polymerases (*Supplementary Table S4-5*). Dark gray circles indicate strains above our growth threshold while the light-gray circles are strains below the growth threshold. (**D**) Cumulative frequency of all *ps* of the proteasome and the three RNA polymerases. All competition effects were excluded. We indicate the prey-bait combinations that are perturbed by the duplication of *PRE7*. (**E**) Relationship between the selection coefficient and the average *ps* (absolute value) of duplicated subunits on PPIs. Only significant (FDR, *q-value* < *0.05*) and non-competition instances were used to calculate the averages. Circles represent duplications of proteasome subunits, while triangles represent subunits of any of the three RNA polymerases. In red we show Pearson's correlation coefficient.

Most proteasome subunits have an attenuated expression level when duplicated

Our experiments indicate that most PPIs within the proteasome interaction network and RNA polymerases are not significantly perturbed after duplication of their subunits. This suggests that these protein complexes are resilient to changes in gene-dosage of their components. Because we observed one of the strongest *ps* in the case of the proteasome, we focused on this complex to explore the underlying mechanisms of such robustness. It has been reported in multiple studies that transcription is usually correlated with gene copy number while protein abundance correlates more poorly. Therefore, regulation mechanisms reducing the protein abundance of the proteasome subunits, also known as attenuation, could explain why duplication is not perturbing PPI between the subunits. To test if the proteasome subunits are attenuated, we looked for changes in protein abundance before and after gene duplication. We measured protein abundance of proteasome subunits in GFP-tagged strains (Huh et al., 2003), carrying a duplication of the gene with the GFP fusion or simply transformed with the empty vector as a control (Figure 3A). Protein attenuation would lead to a reduction of protein levels of both copies, which would result in reduced fluorescence signal. Most subunits have a significant decrease in GFP-fluorescent signal after duplication (Figure 3B; *Supplementary Table S5*).

We calculated an attenuation score: the difference between *WT* and the duplicated GFP-fluorescent signals normalized by the *WT* (Figure 3C). The attenuation score is larger for the highly expressed subunits, as we found that the expression difference between the duplicated and control strain is highly correlated with the abundance of the subunit in the control (Figure 3D). This trend was also observed while comparing with protein expression data from previous studies, including more sensitive approaches (*Supplementary Figure S5*). This suggests that this regulatory mechanism is responsive to the amount of extra gene-product in the cell. We further explored this by using a tunable expression system to measure attenuation at different expression levels of *PRE7*, one of the most attenuated subunits. We constructed a strain with tunable *PRE7* expression (Aranda-Díaz et al., 2017); the strain used for this assay contains two gene copies of *PRE7* tagged with different fluorescent proteins that were monitored by flow cytometry. We found that there is a highly significant negative correlation (*Pearson's correlation* $r = -0.26$, $p < 10e-15$) between the protein abundance of the copy expressed under the inducible promoter and abundance of the chromosome copy (*Supplementary Figure S6, TableS8*). These results suggest that attenuation increases with expression level to maintain specific protein levels in the cell.

We compared the attenuation score across the different proteasome subcomplexes (Figure 3E). Interestingly, attenuation is similar for subunits belonging to the same subcomplex. Havugimana *et* al. (Havugimana et al., 2012) reported that the stoichiometry within each proteasome subcomplex is 1:1, while the stoichiometry among subcomplexes varies from 1:1 to 1:4 (*Supplementary Table S6*). This observation could explain why subunits belonging to the same component have similar expression and attenuation patterns, while there are significant differences between components (Figure 3E; $p = 0.002$ *one-way ANOVA Test*). Furthermore, this highlights the contribution of attenuation to the control of the stoichiometry among the subunits of the proteasome complex.

Figure 3

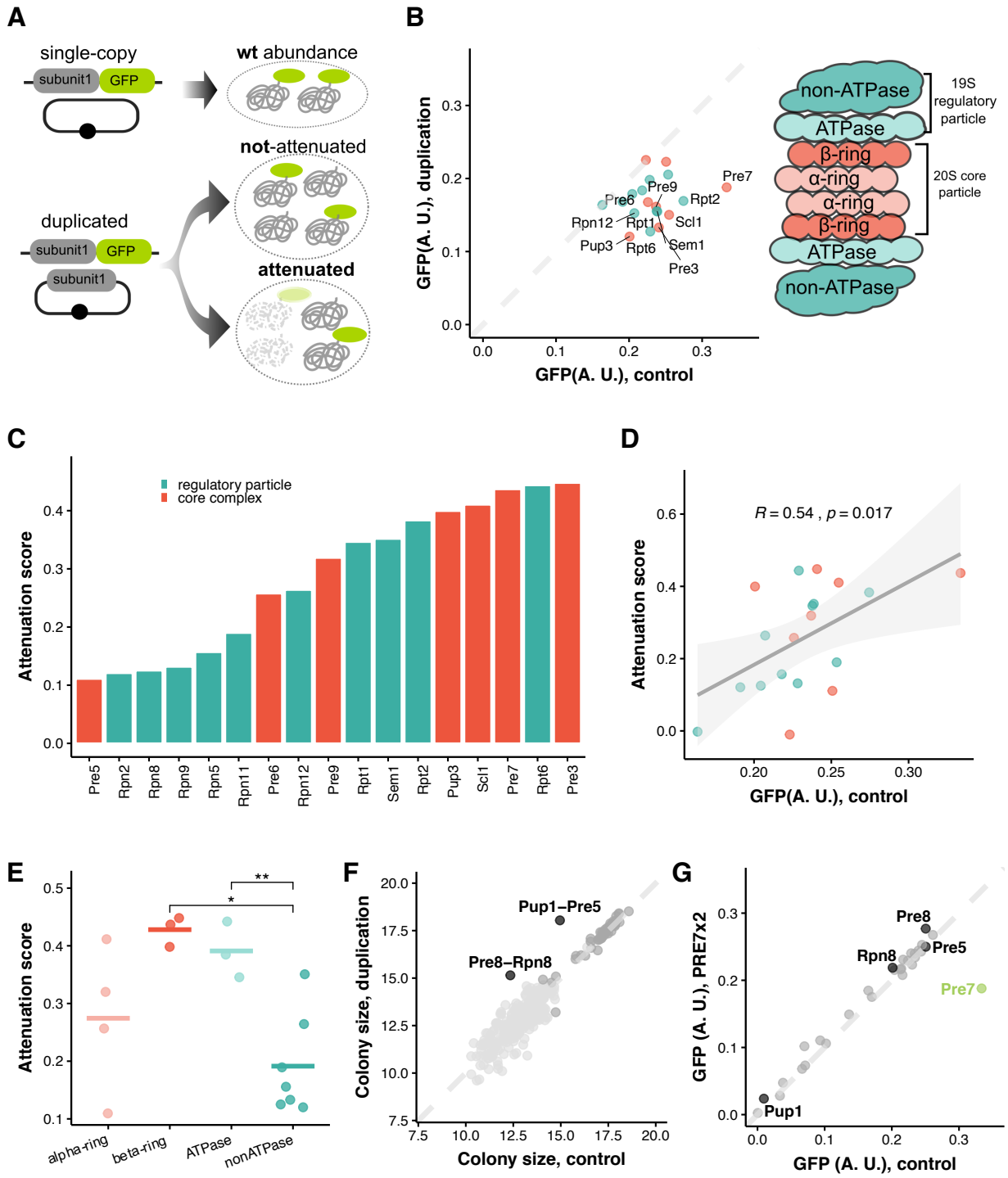

Figure 3. **Attenuation of protein abundance after duplication in most proteasome subunits**. **(A)** Measuring attenuation with GFP-tagged proteins. Changes in abundance of each subunit can be detected by comparing fluorescent signals of GFP-tagged subunits before and after duplication. (**B**) GFP signal comparison between strains carrying a duplication of the GFP-tagged subunit and their corresponding control. On the right, a cartoon of the proteasome with its components. All GFP values are corrected for autofluorescence by subtracting the signal of the parental strain not expressing GFP and by

cell size (see Methods, *Supplementary TableS6*) (**C**) Attenuation scores of all assayed proteasome subunits. The attenuation score is the difference between GFP fluorescent signals of the control strain (bearing a control plasmid) and the duplicated strain (bearing a centromeric plasmid with an extra copy of the subunit) divided by the GFP signal of the control. (**D**) Correlation between attenuation-score and the *WT* fluorescence signal. On the bottom, Pearson's correlation and p-value. (**E**) Comparison of attenuation scores between each proteasome subcomplex. On the right, the asterisks indicate significant differences between components calculated by correcting for multiple testing (*Tukey's test; * $p \leq 0.05$ and ** $p \leq 0.01$*). (**F**) Colony sizes of all strains carrying the *PRE7* duplication (+*pCEN-PRE7*) compared with their control strain (the empty vector). The black dots highlight the subunits that have interactions disturbed after *PRE7* duplication. (**G**) GFP signal of proteasome subunits before and after *PRE7* duplication (+*pCEN-PRE7*). The black dots highlight the subunits that have interactions disturbed after *PRE7* duplication (*Supplementary TableS7*).

One of the most attenuated subunits is Pre7p, a subunit that has one of the strongest effects on both PPIs and fitness when duplicated (Figure 2D-E). The duplication of *PRE7* perturbs PPIs between other subunits of the proteasome, namely Pre5p, Pre8p, Pup1p, and Rpn8p (Figure 3F). All of them share close spatial proximity with Pre7p in the proteasome core complex. We tested if *PRE7* duplication affects the abundance of other subunits by measuring the GFP signal of all proteasome subunits with and without *PRE7* duplication. Most subunits are unaffected upon *PRE7* duplication which further confirms that the attenuation observed in other proteasome subunits is not achieved by the duplication of any proteasome subunit but the subunit that is fused with GFP. Interestingly, we find that the four 'perturbed' subunits (Pre5p, Pre8p, Pup1p, and Rpn8p) show a modest increase in their protein abundance (Figure 3G). To validate these differences, we repeated this experiment using 12 independent biological replicates. Even though the difference between control and *PRE7* duplicated background is small, it is highly reproducible and significant (Wilcoxon rank-sum test results are shown in Supplementary Figure S7A). As a control group, we performed this experiment on four other subunits that are not perturbed by *PRE7* duplication; we found that the difference is not significant in those instances (*Supplementary Figure S7B*). These modest but significant changes in protein abundance of 'perturbed' subunits after the duplication of *PRE7* may explain the changes we observed in their PPIs. The duplication of *PRE7*, even if largely attenuated, affects the organization of the proteasome by affecting the abundance and interactions of a few other subunits.

Recent studies in aneuploid cells (Chen et al., 2019; Dephoure et al., 2014) suggest that attenuation occurs at the posttranscriptional level. To test this, we retrieved data from (Dephoure et al., 2014). In this genome-wide screening, they estimated a mRNA abundance ratio of individual genes in aneuploid strains relative to wild-type (*WT*). Most proteasome's subunits roughly double their transcript levels when duplicated (18/23 relative mRNA ratio >1.5; *Supplementary Figure S8A*). Since aneuploidies can cause systemic level changes on the transcriptome and confound the effects of an individual duplication, we further tested this result using a different approach, using centromeric constructions that contain *PRE7*'s full promoter and ORF but that cannot be translated because it lacks a start codon or the start codon is followed by stop codons. While both the promoter and the rest of the ORF are intact, Pre7p remains at the *WT* level of expression in the presence of these three constructions, showing that attenuation is likely not regulated at a transcriptional level (*Supplementary Figure S9*). Finally, to explore the possibility of feedback attenuation at the translational level, we compared the synthesis rates of Pre7p from disomic cells estimated by (Taggart & Li, 2018). In this work, the authors use ribosome profiling to estimate synthesis rates across the whole proteome of yeast aneuploid strains. Their data indicates that Pre7p synthesis rates scale accordingly with gene copy number, as is the case for most proteasome subunits (*Supplementary Figure S8B*). These results suggest that the

regulatory mechanism that controls attenuation is neither transcriptional nor translational and is, therefore, posttranslational.

Discussion

The long-term fate of gene duplicates has been studied in detail theoretically, experimentally and by using genome, transcriptome, and proteome data. While less is known about the immediate impact of gene duplication, it has become clear that dosage sensitivity determines whether gene duplications have any chance to be retained and fix in a population (Rice & McLysaght, 2017a). By duplicating 899 genes individually and examining the distribution of fitness effects, we find that duplicates with a greater than 1% fitness effect are common (~12%). Furthermore, duplications are twice as likely to be deleterious than beneficial, and deleterious effects are larger in magnitude. Consistent with previous observations, deleterious duplications are more frequent among genes that are also sensitive to a reduction in gene dosage. To test whether these deleterious effects impact fitness by affecting PPIs in protein complexes, we measured the perturbation of protein complexes *in vivo* as a response to gene duplication, focusing on the proteasome and three RNA polymerases. Overall, only 0.24% of the tested duplication-PPI combinations significantly perturbed their protein complexes, and a single subunit largely drives these results. By focusing on the proteasome, we further examined why so few PPIs were perturbed by changes in gene dosage and found that most of its subunits are attenuated at various extents, i.e. the protein level decreases close to a normal level even if the gene is duplicated or its expression is modified with a tunable promoter. Therefore, our results suggest that gene duplication is unlikely to have an impact on fitness through the perturbation of protein complex assembly because extra copies of the proteins are degraded. Altogether, these observations challenge the gene balance hypothesis, support a model in which decreased dosage mainly affects protein complexes (Semple et al., 2008), and identify the mechanism explaining the discrepancy between the effects of decreased and increased dosage.

We found one clear exception to this pattern: the duplication of *PRE7* is highly deleterious and affects PPIs. Further experiments suggest that these alterations are a result of changes in protein abundance of other subunits, which may occur through stabilizing interactions. In previous experiments where we combined gene deletion with the study of PPIs, we documented several cases of protein destabilization by the deletion of an interaction partner (Diss et al., 2013, 2017). What we see here could be the reciprocal effect. Given that Pre7 is one of the most abundant subunits, attenuation may not be sufficient to eliminate the effects of its duplication.

Attenuation of multi-protein complex members has been documented previously in overexpression experiments (Ishikawa et al., 2017), in aneuploid yeast strains (Chen et al., 2019; Dephoure et al., 2014), and to some extent in cancer cells (Gonçalves et al., 2017), which may suffer from a general alteration of protein homeostasis and protein quality control (Oromendia & Amon, 2014). Here we show that attenuation is also taking place with small copy-number variation affecting individual genes, such as in the case of gene duplication. This feature appears to be part of the regulation of proteins in normal cells. Indeed, a recent study by Taggart *et al*. (2020) suggested that nearly 20% of proteasome proteins are overproduced since more than half of the protein synthesized is degraded in normal conditions. Therefore, our results suggest that mechanisms acting to regulate protein abundance in normal conditions provide, as a side effect, the extra advantage of protecting the cell against copy-number variation of some members of important multi-protein complexes. In the case of aneuploid cells and protein overexpression, several mechanisms for the attenuation of protein levels have been proposed such as autophagy, the HSF1/HSP90 pathway (Donnelly et al., 2014; Oromendia et al., 2012), and the ubiquitin-

proteasome system (Dephoure et al., 2014; Ishikawa et al., 2017; Stingele et al., 2012; Torres et al., 2010). Since the proteasome itself may play an essential role in attenuation, studying the mechanism of attenuation in this complex may prove to be challenging. Nevertheless, the mechanisms protecting the cells of the proteotoxic stress caused by aneuploidy may not be the same that act in the case of small-scale duplications. The molecular mechanisms that attenuate protein abundance in the case of individual gene duplications are still an open question.

Our observations, along with those of previous studies, have an important impact on our understanding of the evolution of protein complexes. Complexes are often composed of multiple pairs of paralogs (Musso et al., 2007; Pereira-Leal et al., 2007), particularly but not exclusively, those coming from a whole-genome duplication (WGD). The relationship between WGD and the retention of gene duplicates in protein complexes has often been explained by a model in which the deleteriousness of single duplications comes from the alteration of protein stoichiometry, which is not affected upon WGD. However, cells appear to have mechanisms to maintain the stoichiometry of at least some protein complexes, which means that the cost of duplication would not come from the perturbation of stoichiometry, but rather from the degradation of excess proteins. It is difficult to imagine that such cost, rather than perturbations of stoichiometry, would explain the observation that complex subunits are more likely to be retained after a WGD event, but are less likely to be duplicated individually (Qian & Zhang, 2008). This explanation, therefore, needs further examination and the extension of the study of attenuation to a larger number of complexes.

Evolutionary forces leading to regulatory mechanisms that attenuate protein abundance, therefore, diminish the immediate fitness effects of gene duplications and could allow them to reach a higher frequency in populations. Such pressures could come, for instance, from a constant requirement to assemble protein complexes in a stoichiometric fashion in the face of gene expression noise (Fraser et al., 2004). Another pressure for the degradation of extra-subunits is the need to prevent spurious interactions between the unassembled subunits and other proteins through its exposed sticky interface (Levy et al., 2012) or aggregation (Brennan et al., 2019). If selection for decreasing noise or to reduce spurious interactions led to the evolution of protein attenuation, it may have also contributed to the robustness of protein complexes to gene duplications. Then, if the cost of producing extra RNA and protein is not too high, newly arisen duplicated subunits would have a higher probability of fixation and of long-term maintenance, perhaps by dosage subfunctionalization (Gout & Lynch, 2015).

Material and methods

Parental strains, media, and plasmids for the fitness measurements

We extracted the MoBY plasmids from bacteria using a 96-well plate miniprep extraction by alkaline lysis (Engebrecht et al., 1991). The parental strain used for the fitness assay library is Y8205-mCherry (*MATα ho::PDC1pr-mCherry-hphMX4 can1Δ::STE2pr-Sp_his5 lyp1Δ::STE3pr-LEU2 his3Δ1 leu2Δ0 ura3Δ0*), a modification of the Y8205 strain from (Tong & Boone, 2006) done by Garay et al. (2014). The reference strain used for the competition fitness assay was Y7092-CFP (*MATα hoΔ::Cerulean-natR can1Δ::STE2pr-SP_his5 lyp1Δ Δhis3Δ1 leu2Δ0 ura3Δ0 met15Δ0 LYS2*+) transformed with a control plasmid (p5586; (Ho et al., 2009)) identical to those from the MoBY-ORF Collection but without yeast-gene sequence. To generate the collection with duplication of essential genes, we used a high-efficiency yeast transformation method for 96-well format (Dan Burke et al., 2000). To select positive transformants we incubated plates at 30 °C for 3-5 days and cherry-picked two colonies per sample. The competition medium was a minimal low-fluorescence synthetic medium without uracil (SC[MSG]-lf -ura, *Supplementary Table S10*).

Measurements of relative fitness by fluorescence-based competition assays

To measure relative fitness we used an automated high-resolution method based on fluorometry previously developed by (DeLuna et al., 2008). The mCherry-tagged collection carrying individual 'duplications' (Y8205-mCherry+MoBY-xxx) were competed with a universal CFP-tagged strain (Y7092-CFP +p5586). First, we inoculate 150 µL of fresh competition medium (using Corning® Costar® 96-well cell culture plates) with overnight cultures of 'duplicated' and reference strains (tagged with mCherry and CFP respectively) in a 1:2 proportion. Every 24 h, we diluted the cultures 16-fold into sterile fresh competition media. Cultures were monitored in parallel for approximately 28 generations (7 days) in a fully automated robotic system (Freedom EVO, Tecan Ltd) connected with a microplate multi-reader (Infinite Reader M100, Tecan Ltd). We monitored OD600 nm, mCherry fluorescence signal (578/610 nm, gain: 145), and CFP fluorescence signal (433/475 nm, gain: 120) every 2 h. Cultures were incubated at 30 °C and 70 % relative humidity.

Estimation of selection coefficients

We estimated the selection coefficient by measuring the change in population ratios of cells carrying a duplication (mCherry signal) on the reference strain (CFP signal), following the standard procedures developed by (DeLuna et al., 2008). Each fluorescent signal was corrected for media autofluorescence and for the crosstalk between fluorescent signals. To calculate each fluorophore crosstalk, we measured $mCherry_{BKG}$ background signal in CFP-only wells and CFP_{BKG} in mCherry-only wells. Then, we subtracted the background signals: mCherry = $mCherry_{RAW}$-$mCherry_{BKG}$ and CFP = CFP_{RAW}-CFP_{BKG}. Corrected fluorescence values were used to estimate *ln(mCherry/CFP)* ratios for all measurement points. Then, we interpolated a single ratio per dilution cycle at a fixed OD600nm (0.2) to reduce artifacts related to the dependence between the fluorescent signals. We discarded any extreme ratios (*ln(mCherry/CFP)* > 4 or < -4) and samples with less than three data points. We calculated the selection coefficients using the equation:

$$s = \frac{d}{dt}\left[\frac{ln(mCherry/CFP)}{log2}\right] = 1 - W$$

Where: ***s*** is the selection coefficient, ***t*** is the number of generations, and ***W*** is relative fitness. We normalized each *s* using the median of the complete distribution of strains. We calculated z-score using the mean and the standard deviation of a control distribution of 192 Cherry-tagged *WT* strains competed against the universal CFP-tagged reference. All calculations were performed using scripts written in MatLab and in R.

Measurements of relative fitness by cytometry-based competition assays
The Y8205-mCherry +MoBY-xxx collection was co-cultured with a universal YFP-tagged strain (Y7092-YFP +p5586). Daily dilutions steps were carried in the same conditions and with the same automated equipment as the fluorescence-based competition assays. Before each dilution, we took a sample of 10 µL of saturated culture and made a 1:10 dilution in TE 2X (*Supplementary Table S10*) in 96-well plates. For cell cytometry measurements, we used the LSRFortessa™(BD, USA) cytometer. We collected up to 30,000 events using the integrated high-throughput sampler. We calculated the number of cells expressing mCherry or YFP fluorescence using the FACSDiva™ (BD, USA) software tool for manual gating. Selection coefficient estimation was done using the same equation as in the fluorescence experiments with custom MatLab and R scripts.

Generation of DHFR-PCA strain library with duplicated subunits
We retrieved strains that contain DHFR fragment fusions of subunits of the proteasome, RNA polymerase I, II, and II from the Yeast Protein Interactome Collection (Tarassov et al., 2008). We confirmed the correct insertion of the DHFR fragments by colony PCR using an ORF specific forward Oligo-C (Giaever et al., 2002) located upstream of the fusion and a universal reverse complement oligonucleotide ADHterm_R. PCR amplicons were sequenced to confirm correct fusion with the DHFR fragments. All oligonucleotide sequences can be found in *Supplementary Table S9*. PCR reaction conditions and reagents are the same as in (Marchant et al., 2019). The numbers of confirmed DHFR strains are indicated in *Supplementary Table S4*.

The 70 plasmids that were retrieved from the MoBY ORF Collection (Ho et al., 2009) contain subunits from the Retromer (6), Proteasome (33), and RNA polymerases I, II and II (31) (see *Supplementary Table S4)*. We confirmed their identities using Oligo-C and a universal plasmid-specific oligo KanR (*Supplementary Table S9*). All plasmids were extracted using Presto Mini Plasmid Kit (Geneaid Biotech Ltd, Taiwan).

The strains expressing DHFR fusions and an additional gene copy from the MoBY plasmids or the empty plasmid were transformed following a standard technique (Dan Burke et al., 2000). The selection was done in three steps. The first round was done in 96l deep-well plates in 800 µL of SD[MSG] -ura, incubated for 2 d at 30°C with shaking. The second round was done by inoculating 5 µL of the first-round selection cultures into 800 µL of fresh selection media. Finally, cells were printed on agar plates with double selection SD[MSG] -ura + G418 (200 mg/mL).

We took all confirmed preys (DHFR-F[3] fusions) and transformed them with all MoBY plasmids available for their complex (*Supplementary TableS4*). We generated 42 strains with the 6 retromer preys each transformed with seven plasmid constructions (6 MoBY-xxx plasmids plus one control plasmid). For the proteasome, 544 strains were constructed by transforming each of the 16 preys with the 34 plasmids (33 MoBY-xxx plasmids and one control plasmid). For the RNA polymerases I, II, and II, we generated 864 strains, 27 preys, and transformed them with 32 plasmids (31 from the MoBY collection and one control plasmid). The control plasmid (pRS316-KanMX) contains the same selection markers as the MoBY plasmids to account for the effect of expressing the markers alone.

DHFR Protein fragment Complementation Assay
DHFR-PCA detects semi-quantitative changes in strength and frequency of the physical interaction between two proteins (Freschi et al., 2013; Levy et al., 2014). This method allows the detection of PPI changes upon perturbations *in vivo*, for instance in response to gene deletion (Diss et al., 2013, 2017; Tarassov et al., 2008). To measure the effect of gene duplication, we introduced an extra copy coded on a centromeric plasmid to simulate gene duplication as above,

and measured changes in the physical interaction between pairs of the complex subunits. The DHFR-PCA screening was performed using standard methods used in previous works (Diss et al., 2017; Marchant et al., 2019; Rochette et al., 2015). All arrays of 96, 384, and 1,536 colonies per plate were manipulated with pin tools controlled by a fully automated platform (BM5-SC1, S&P Robotics Inc., Canada; (Rochette et al., 2015)). Haploid strains were assembled in arrays of 1,536 colonies on agar plates. In order to avoid growth bias at the edge of the agar plates, the border positions (first two and last two columns and rows of each 1,536 array) of all plates were dedicated to positive controls (MAT**a** *LSM8*-DHFR-F[1,2] and MATα *CDC39*-DHFR-F[3]). These two proteins have previously shown a strong interaction in PCA (Marchant et al., 2019).

The complete *MATα prey-DHFR-F[3] +MoBY-xxx* (prey) collection of 1,450 strains was expanded to generate seven independent replicates using a cherry-picking 96-pin tool. Each replica was positioned randomly in the 384-colony array, avoiding border positions. During the cherry-picking step of the preys, we generated 34 plates with 384-colony arrays. We condensed them into 9 plates (one for the retromer, three for the proteasome, and five for the RNA polymerases) of 1,536-colony arrays. All prey manipulations were performed on YPD +hygromycin B (250 mg/L) and G418 (200 mg/mL) media.

For the MAT**a** *bait*-DHFR-F[1,2] (bait) collection, we produced 52 arrays of 1,536 colonies printed on YPD +NAT (100 mg/L) agar plates. On the interior positions, each plate contained the same bait-strain of the Proteasome (21) and the RNA polymerases (31), while in the border positions, we printed the same control strain. In the case of the retromer, six 384-colony arrays were condensed in two plates with 1,536 colonies. As a result, we produced 54 PCA-ready bait plates.

The 9-plate prey collection (MATα *prey*-DHFR-F[3] +MoBY-xxx, Hygromycin B, and G418 resistant) was mated with the set of 54 bait plates (MAT**a** bait-DHFR-F[1,2], NAT resistant). All crosses were performed within each complex in the following manner: for the retromer prey plate was crossed with 2 bait plates, generating 2 mating plates. For the proteasome, three prey plates were crossed with 21 bait plates, generating 63 mating plates. Finally, for the RNA polymerases, each of the five prey plates was crossed with the 31 corresponding baits, resulting in 155 mating plates. Mating was done on agar plates of YPD and incubated at room temperature for 2 d. Then, we replicated the set of 220 mating plates on diploid selection media containing the three antibiotics (YPD +hygromycin B (250 mg/L), NAT (100 mg/L), and G418 (200 mg/mL) and incubated the plates at 30 °C for 48 h. We repeated this step to improve colony homogeneity. Finally, the complete set of diploids was replicated on both DMSO and MTX media (*Supplementary Table S10*) two consecutive times, each step with incubation at 30 °C for 96 h. We monitored growth in the last step of both DMSO and MTX selections. We captured images of the plates every 24 h using a Rebel T5i camera (Canon, Tokyo, Japan) attached to our robotic system (S&P Robotics Inc, Toronto, Canada).

Data Analysis of the DHFR-PCA screening

We used a plate image analysis method to measure colony sizes as the integrated pixel density of each position of the 1,536-array plates. Plate pictures were processed by a customized pipeline that was implemented using the ImageJ 1.45 (http://rsbweb.nih.gov/ij/) software as described previously by (Diss et al., 2013, 2017). We calculated a PPI-score for each position by subtracting colony size on the control medium (DMSO) to the colony size on the DHFR selective media (MTX) to eliminate any fitness or position bias. Then, we calculated a mean PPI score by averaging the specific interaction scores of the seven biological replicas. We used the R function 'normalmixEM()' (Benaglia et al., 2009) to adjust the PPI scores to a bimodal distribution. This

model was used to determine a PPI score threshold of 14.7 for positive interactions. We excluded all positions below this threshold and samples with less than five biological replicates, leaving 90% of samples after filtering. We calculated *ps* as the difference of PPI scores between 'duplicated' (+MoBY-xxx) and *WT* (+pRS316-KanMX) background. We estimated statistical significance with a two-sided paired Student's T-test. The resulting p-values were then adjusted (to q-values) for multiple comparisons using the FDR method (Benjamini & Yekutieli, 2001) with the p.adjust() function in R. Samples with q-values below 0.05 were considered positive hits. All the analysis pipeline was done using custom R scripts.

Measurements of protein abundance by flow cytometry

We used GFP(S65T)-HIS3MX–tagged strains from the Yeast GFP fusion Collection (Huh et al., 2003). The identities of the 33 strains expressing GFP-tagged proteasome subunits were confirmed by colony PCR using an ORF specific oligo (*Supplementary Table S9*). We generated *de novo* GFP-fusions for four subunits (*PRE7*, *RPT2*, *PRE1*, and *PUP3*) that were not present in the Yeast GFP Fusion Collection. These fusions were produced following the same strategy described in the original work (Huh et al., 2003). We confirmed at least one clone of each new GFP-tagged construction by cytometry, colony PCR, and sequencing (*Supplementary Table S9*). Each GFP-tagged strain was transformed with a plasmid of the MoBY ORF library expressing an additional gene-copy of the same tagged subunit. Since there are only 33 subunits present on the MoBY ORF library, therefore, attenuation could only be measured for the corresponding proteins.

For the cytometry measurements, we inoculated the strains in a 96 deep-well plate in 500 µL of SD[MSG] -ura -his media. The plate was sealed with a sterile breathable membrane. After overnight growth at 30 °C (with shaking), the saturated culture was diluted 1:10 in the same media. Cells were incubated again for 4-6 hours at 30 °C with agitation. Then, cells in exponential phase were diluted in sterile ddH_2O to an approximate concentration of 500 cells/µL. The GFP fluorescence of 5000 cells was measured using a Guava easyCyte 14HT BGV flow Cytometer (Millipore, USA). All data processing was done using custom R scripts. Events with FSC-H or SSC-H values below 1000 were discarded. The GFP signal for each event was normalized with cell size using FSC-A value. Finally, we subtracted the autofluorescence value of the cells, calculated by measuring the parental BY4741 strain without any fluorescent protein. For further analysis, we only considered strains with GFP signals above the median plus 2.5 standard deviations of the *WT* non-GFP strain.

Attenuation experiments with an estradiol inducible promoter system.

To construct the inducible promoter plasmid, we cloned *PRE7* in the pAG416GAL-ccdB-EGFP plasmid (Addgene plasmid # 14195). To generate this construction, we amplified *PRE7* (ORF only) from the strain BY4741 genomic DNA using oligonucleotides listed in *Supplementary Table S9* that contain gateway attR recombination sequences. We used 300 ng of purified PCR product to set a BPII recombination reaction (5 µL) into the Gateway Entry Vector pDONR201 (150 ng) using the standard methods provided by the manufacturer (Invitrogen, USA). BPII reaction mix was incubated at 25 °C overnight. The reaction was inactivated with proteinase K. The 5 µL reaction was used to transform MC1061 competent *E. coli* cells. The selection was performed in 2YT + 50 mg/L of kanamycin (BioShop Inc, Canada) at 37 °C. Positive clones were detected by PCR using an ORF specific oligonucleotide and a general pDONR201 primer (*Supplementary Table S9*). We isolated plasmid from one positive clone that was confirmed both by PCR and by Sanger sequencing. The LRII reaction was performed mixing 150 ng of pDONR201-PRE7 and 150 ng of pAG416GAL-ccdB-EGFP. The reaction was incubated overnight at 25°C and inactivated with proteinase K. The reaction was used to transform MC1061 competent *E. coli* cells, followed by selection on solid 2YT + 100 mg/L ampicillin (BioShop Inc, Canada) at 37°C. Positive clones were confirmed by PCR and Sanger sequencing using *PRE7* and pG416GAL-

ccdB-EGFP specific oligonucleotides (*Supplementary TableS9*). The sequence-verified pAG416GAL-PRE7-EGFP plasmid was used to transform the yeast strain *PRE7*-mKate (BY4741 MATa *Δhis3 Δura3 Δmet15 LEU2::GEM PRE7-mKate-hph*) using a lithium acetate standard protocol. As a reference, we transformed the same parental strain with the empty expression plasmid pG416GAL-ccdB-EGFP. The selection of positive transformants was done on SC[MSG] -ura -leu for 3 days at 30°C.
For the induction experiments, we set up overnight cultures of the PRE7-mKate + pAG416GAL-PRE7-EGFP strain and the reference (*PRE7*-mKate + pG416GAL-ccdB-EGFP) in 5 mL of SC[MSG] -ura -leu. We diluted the saturated culture 1:10 in 96-well plates containing 200 µL of SC[MSG] -ura -leu containing Estradiol (β-estradiol, Sigma-Aldrich) at different concentrations (0, 6.25, 12.5, 25, 50 and 100 nM). We incubated at 30°C with shaking for 12 hours. Then, cells in exponential phase were diluted in sterile ddH_2O to an approximate concentration of 500 cells/µL, and mKate and GFP fluorescence signal was measured as described previously.

Mutagenesis of MoBY-PRE7 plasmid
To generate MoBY-PRE7 plasmids without translation of Pre7p, we performed site-directed mutagenesis. For a 25 µL mutagenesis reaction, the following were mixed: 5 µL Kapa HiFi buffer 5X (Kapa Biosystems, USA), 0.75 µL dNTPs 10 µM, 0.75 µL forward oligonucleotide 10 µM, 0.75 µL reverse oligonucleotide 10 µM (see *Supplementary Table S9*), 0.5 µL Kapa hot-start polymerase (Kapa Biosystems, USA), 0.75 µL MoBY-PRE7 plasmid DNA (15 ng/µL), 16.5 µL PCR grade water. The following thermocycler protocol was then used: 95 °C for 5 min, then 20 cycles of 98 °C for 20 s, 60 °C for 15 s, 72 °C for 11 min and then 72 °C for 15 min. The PCR product was digested with DpnI for 2 h at 37 °C and 5 µL was transformed in *E. coli* strain BW23474 (F−, Δ*(argF-lac)169*, Δ*uidA4::pir-116*, *recA1*, *rpoS396 (Am)*, *endA9(del-ins)::FRT*, *rph-1*, *hsdR514*, *rob-1*, *creC510*). Transformation reactions were spread on agar plates of 2YT media with Kanamycin (50 µg/mL) and Chloramphenicol (12.5 µg/mL) and grown at 37 °C overnight. Three independent colonies were isolated from each transformation and confirmed by sequencing.

Databases used for data analysis
The list of genes that code for members of multi-protein complexes of *S. cerevisiae* (S288c) was obtained from the Complex Portal (https://www.ebi.ac.uk/complexportal/home) developed and maintained by (Meldal et al., 2019).
Protein abundance data were extracted from the latest update for *S. cerevisiae* of the PaxDB database (https://pax-db.org/; (Wang et al., 2012). Haploinsufficient genes were taken from the work of (Deutschbauer et al., 2005).

Acknowledgments
We thank E. Mancera and members of the Landry and DeLuna labs for discussions and comments on the manuscript. This research was supported by a CIHR Foundation grant to CRL (387697) and by CONACYT México through grants CB-2015/164889 and PN-2016/2370 to AD. CRL holds the Canada Research in Cellular Synthetic and Systems Biology.

Abbreviations

DHFR	Dihydrofolate Reductase
GFP	Green Fluorescent Protein
FDR	False Discovery Rate
PCA	Protein Complementation Assay
pCEN	Centromeric Plasmid
PPIs	Protein-protein Interactions
ps	Perturbation Score
s	Selection Coefficient
WGD	Whole-genome Duplication
WT	Wild type

References

Aranda-Díaz, A., Mace, K., Zuleta, I., Harrigan, P., & El-Samad, H. (2017). Robust Synthetic Circuits for Two-Dimensional Control of Gene Expression in Yeast. *ACS Synthetic Biology*, *6*(3), 545–554.

Archambault, J., & Friesen, J. D. (1993). Genetics of eukaryotic RNA polymerases I, II, and III. *Microbiological Reviews*, *57*(3), 703–724.

Benaglia, T., Chauveau, D., Hunter, D. R., & Young, D. (2009). mixtools : An R Package for Analyzing Finite Mixture Models. *Journal of Statistical Software*, *32*(6). https://doi.org/10.18637/jss.v032.i06

Benjamini, Y., & Yekutieli, D. (2001). The Control of the False Discovery Rate in Multiple Testing under Dependency. *Annals of Statistics*, *29*(4), 1165–1188.

Birchler, J. A., & Veitia, R. A. (2007). The gene balance hypothesis: from classical genetics to modern genomics. *The Plant Cell*, *19*(2), 395–402.

Brennan, C. M., Vaites, L. P., Wells, J. N., Santaguida, S., Paulo, J. A., Storchova, Z., Harper, J. W., Marsh, J. A., & Amon, A. (2019). Protein aggregation mediates stoichiometry of protein complexes in aneuploid cells. *Genes & Development*, *33*(15-16), 1031–1047.

Broek, D., Toda, T., Michaeli, T., Levin, L., Birchmeier, C., Zoller, M., Powers, S., & Wigler, M. (1987). The S. cerevisiae CDC25 gene product regulates the RAS/adenylate cyclase pathway. *Cell*, *48*(5), 789–799.

Budenholzer, L., Cheng, C. L., Li, Y., & Hochstrasser, M. (2017). Proteasome Structure and Assembly. *Journal of Molecular Biology*, *429*(22), 3500–3524.

Burke, D., Dawson, D., & Stearns, T. (2000). *Methods in Yeast Genetics: A Cold Spring Harbor Laboratory Course Manual*. CSHL Press.

Burke, D., Gasdaska, P., & Hartwell, L. (1989). Dominant effects of tubulin overexpression in Saccharomyces cerevisiae. *Molecular and Cellular Biology*, *9*(3), 1049–1059.

Chen, Y., Chen, S., Li, K., Zhang, Y., Huang, X., Li, T., Wu, S., Wang, Y., Carey, L. B., & Qian, W. (2019). Overdosage of Balanced Protein Complexes Reduces Proliferation Rate in Aneuploid Cells. *Cell Systems*, *9*(2), 129–142.e5.

Chrétien, A.-È., Gagnon-Arsenault, I., Dubé, A. K., Barbeau, X., Després, P. C., Lamothe, C., Dion-Côté, A.-M., Lagüe, P., & Landry, C. R. (2018). Extended Linkers Improve the Detection of Protein-protein Interactions (PPIs) by Dihydrofolate Reductase Protein-fragment Complementation Assay (DHFR PCA) in Living Cells. *Molecular & Cellular Proteomics: MCP*, *17*(2), 373–383.

Cramer, P. (2002). Multisubunit RNA polymerases. *Current Opinion in Structural Biology*, *12*(1), 89–97.

DeLuna, A., Vetsigian, K., Shoresh, N., Hegreness, M., Colón-González, M., Chao, S., & Kishony, R. (2008). Exposing the fitness contribution of duplicated genes. *Nature Genetics*, *40*(5), 676–681.

Dephoure, N., Hwang, S., O'Sullivan, C., Dodgson, S. E., Gygi, S. P., Amon, A., & Torres, E. M. (2014). Quantitative proteomic analysis reveals posttranslational responses to aneuploidy in yeast. *eLife*, *3*, e03023.

Deutschbauer, A. M., Jaramillo, D. F., Proctor, M., Kumm, J., Hillenmeyer, M. E., Davis, R. W., Nislow, C., & Giaever, G. (2005). Mechanisms of haploinsufficiency revealed by genome-wide profiling in yeast. *Genetics*, *169*(4), 1915–1925.

Diss, G., Dubé, A. K., Boutin, J., Gagnon-Arsenault, I., & Landry, C. R. (2013). A systematic approach for the genetic dissection of protein complexes in living cells. *Cell Reports*, *3*(6), 2155–2167.

Diss, G., Gagnon-Arsenault, I., Dion-Coté, A.-M., Vignaud, H., Ascencio, D. I., Berger, C. M., & Landry, C. R. (2017). Gene duplication can impart fragility, not robustness, in the yeast protein interaction network. *Science*, *355*(6325), 630–634.

Donnelly, N., Passerini, V., Dürrbaum, M., Stingele, S., & Storchová, Z. (2014). HSF 1 deficiency and impaired HSP 90-dependent protein folding are hallmarks of aneuploid human cells. *The EMBO Journal*, *33*(20), 2374–2387.

Engebrecht, J., Brent, R., & Kaderbhai, M. A. (1991). Minipreps of Plasmid DNA. *Current Protocols in Molecular Biology / Edited by Frederick M. Ausubel ... [et Al.]*, *15*(1). https://doi.org/10.1002/0471142727.mb0106s15

Espinet, C., de la Torre, M. A., Aldea, M., & Herrero, E. (1995). An efficient method to isolate yeast genes causing overexpression-mediated growth arrest. *Yeast* , *11*(1), 25–32.

Fischer, M., Hilt, W., Richter-Ruoff, B., Gonen, H., Ciechanover, A., & Wolf, D. H. (1994). The 26S proteasome of the yeast Saccharomyces cerevisiae. *FEBS Letters*, *355*(1), 69–75.

Fraser, H. B., Hirsh, A. E., Giaever, G., Kumm, J., & Eisen, M. B. (2004). Noise minimization in eukaryotic gene expression. *PLoS Biology*, *2*(6), e137.

Freschi, L., Torres-Quiroz, F., Dubé, A. K., & Landry, C. R. (2013). qPCA: a scalable assay to measure the perturbation of protein-protein interactions in living cells. *Molecular bioSystems*, *9*(1), 36–43.

Garay, E., Campos, S. E., González de la Cruz, J., Gaspar, A. P., Jinich, A., & Deluna, A. (2014). High-resolution profiling of stationary-phase survival reveals yeast longevity factors and their genetic interactions. *PLoS Genetics*, *10*(2), e1004168.

Giaever, G., Chu, A. M., Ni, L., Connelly, C., Riles, L., Véronneau, S., Dow, S., Lucau-Danila, A., Anderson, K., André, B., Arkin, A. P., Astromoff, A., El-Bakkoury, M., Bangham, R., Benito, R., Brachat, S., Campanaro, S., Curtiss, M., Davis, K., … Johnston, M. (2002). Functional profiling of the Saccharomyces cerevisiae genome. *Nature*, *418*(6896), 387–391.

Gonçalves, E., Fragoulis, A., Garcia-Alonso, L., Cramer, T., Saez-Rodriguez, J., & Beltrao, P. (2017). Widespread Post-transcriptional Attenuation of Genomic Copy-Number Variation in Cancer. *Cell Systems*, *5*(4), 386–398.e4.

Gout, J.-F., & Lynch, M. (2015). Maintenance and Loss of Duplicated Genes by Dosage Subfunctionalization. *Molecular Biology and Evolution*, *32*(8), 2141–2148.

Havugimana, P. C., Hart, G. T., Nepusz, T., Yang, H., Turinsky, A. L., Li, Z., Wang, P. I., Boutz, D. R., Fong, V., Phanse, S., Babu, M., Craig, S. A., Hu, P., Wan, C., Vlasblom, J., Dar, V.-U.-N., Bezginov, A., Clark, G. W., Wu, G. C., … Emili, A. (2012). A census of human soluble protein complexes. *Cell*, *150*(5), 1068–1081.

Ho, C. H., Magtanong, L., Barker, S. L., Gresham, D., Nishimura, S., Natarajan, P., Koh, J. L. Y., Porter, J., Gray, C. A., Andersen, R. J., Giaever, G., Nislow, C., Andrews, B., Botstein, D., Graham, T. R., Yoshida, M., & Boone, C. (2009). A molecular barcoded yeast ORF library enables mode-of-action analysis of bioactive compounds. *Nature Biotechnology*, *27*(4), 369–377.

Hochstrasser, M., Johnson, P. R., Arendt, C. S., Amerik, A. Y., Swaminathan, S., Swanson, R., Li, S., Laney, J., Pals-Rylaarsdam, R., Nowak, J., & Others. (1999). The Saccharomyces cerevisiae ubiquitin--proteasome system. *Philosophical Transactions of the Royal Society of London. Series B, Biological Sciences*, *354*(1389), 1513–1522.

Huh, W.-K., Falvo, J. V., Gerke, L. C., Carroll, A. S., Howson, R. W., Weissman, J. S., & O'Shea, E. K. (2003). Global analysis of protein localization in budding yeast. *Nature*, *425*(6959), 686–691.

Ishikawa, K., Makanae, K., Iwasaki, S., Ingolia, N. T., & Moriya, H. (2017). Post-Translational Dosage Compensation Buffers Genetic Perturbations to Stoichiometry of Protein Complexes. *PLoS Genetics*, *13*(1), e1006554.

Iskow, R. C., Gokcumen, O., & Lee, C. (2012). Exploring the role of copy number variants in human adaptation. *Trends in Genetics: TIG*, *28*(6), 245–257.

Katz, W., Weinstein, B., & Solomon, F. (1990). Regulation of tubulin levels and microtubule assembly in Saccharomyces cerevisiae: consequences of altered tubulin gene copy

number. *Molecular and Cellular Biology*, *10*(10), 5286–5294.
Keren, L., Hausser, J., Lotan-Pompan, M., Vainberg Slutskin, I., Alisar, H., Kaminski, S., Weinberger, A., Alon, U., Milo, R., & Segal, E. (2016). Massively Parallel Interrogation of the Effects of Gene Expression Levels on Fitness. *Cell*, *166*(5), 1282–1294.e18.
Levy, E. D., De, S., & Teichmann, S. A. (2012). Cellular crowding imposes global constraints on the chemistry and evolution of proteomes. *Proceedings of the National Academy of Sciences of the United States of America*, *109*(50), 20461–20466.
Levy, E. D., Kowarzyk, J., & Michnick, S. W. (2014). High-resolution mapping of protein concentration reveals principles of proteome architecture and adaptation. *Cell Reports*, *7*(4), 1333–1340.
Li, G.-W., Burkhardt, D., Gross, C., & Weissman, J. S. (2014). Quantifying absolute protein synthesis rates reveals principles underlying allocation of cellular resources. *Cell*, *157*(3), 624–635.
Lynch, M., & Force, A. (2000). The probability of duplicate gene preservation by subfunctionalization. *Genetics*, *154*(1), 459–473.
Marchant, A., Cisneros, A. F., Dubé, A. K., Gagnon-Arsenault, I., Ascencio, D., Jain, H., Aubé, S., Eberlein, C., Evans-Yamamoto, D., Yachie, N., & Landry, C. R. (2019). The role of structural pleiotropy and regulatory evolution in the retention of heteromers of paralogs. *eLife*, *8*. https://doi.org/10.7554/eLife.46754
Meldal, B. H. M., Bye-A-Jee, H., Gajdoš, L., Hammerová, Z., Horácková, A., Melicher, F., Perfetto, L., Pokorný, D., Lopez, M. R., Türková, A., Wong, E. D., Xie, Z., Casanova, E. B., Del-Toro, N., Koch, M., Porras, P., Hermjakob, H., & Orchard, S. (2019). Complex Portal 2018: extended content and enhanced visualization tools for macromolecular complexes. *Nucleic Acids Research*, *47*(D1), D550–D558.
Moriya, H., Makanae, K., Watanabe, K., Chino, A., & Shimizu-Yoshida, Y. (2012). Robustness analysis of cellular systems using the genetic tug-of-war method. *Molecular bioSystems*, *8*(10), 2513–2522.
Mukadam, A. S., & Seaman, M. N. J. (2015). Retromer-mediated endosomal protein sorting: The role of unstructured domains. *FEBS Letters*, *589*(19 Pt A), 2620–2626.
Musso, G., Zhang, Z., & Emili, A. (2007). Retention of protein complex membership by ancient duplicated gene products in budding yeast. *Trends in Genetics: TIG*, *23*(6), 266–269.
Ohno, S. (1970). *Evolution by Gene Duplication*. Springer Berlin Heidelberg.
Oromendia, A. B., & Amon, A. (2014). Aneuploidy: implications for protein homeostasis and disease. *Disease Models & Mechanisms*, *7*(1), 15–20.
Oromendia, A. B., Dodgson, S. E., & Amon, A. (2012). Aneuploidy causes proteotoxic stress in yeast. *Genes & Development*, *26*(24), 2696–2708.
Papp, B., Pál, C., & Hurst, L. D. (2003). Dosage sensitivity and the evolution of gene families in yeast. *Nature*, *424*(6945), 194–197.
Pavelka, N., Rancati, G., Zhu, J., Bradford, W. D., Saraf, A., Florens, L., Sanderson, B. W., Hattem, G. L., & Li, R. (2010). Aneuploidy confers quantitative proteome changes and phenotypic variation in budding yeast. *Nature*, *468*(7321), 321–325.
Pereira-Leal, J. B., Levy, E. D., Kamp, C., & Teichmann, S. A. (2007). Evolution of protein complexes by duplication of homomeric interactions. *Genome Biology*, *8*(4), R51.
Qian, W., & Zhang, J. (2008). Gene dosage and gene duplicability. *Genetics*, *179*(4), 2319–2324.
Qian, W., & Zhang, J. (2014). Genomic evidence for adaptation by gene duplication. *Genome Research*, *24*(8), 1356–1362.
Rice, A. M., & McLysaght, A. (2017a). Dosage sensitivity is a major determinant of human copy number variant pathogenicity. *Nature Communications*, *8*, 14366.
Rice, A. M., & McLysaght, A. (2017b). Dosage-sensitive genes in evolution and disease. *BMC Biology*, *15*(1), 78.

Rochette, S., Diss, G., Filteau, M., Leducq, J.-B., Dubé, A. K., & Landry, C. R. (2015). Genome-wide protein-protein interaction screening by protein-fragment complementation assay (PCA) in living cells. *Journal of Visualized Experiments: JoVE*, *97*. https://doi.org/10.3791/52255

Russell, M., Bradshaw-Rouse, J., Markwardt, D., & Heideman, W. (1993). Changes in gene expression in the Ras/adenylate cyclase system of Saccharomyces cerevisiae: correlation with cAMP levels and growth arrest. *Molecular Biology of the Cell*, *4*(7), 757–765.

Schmitt, H. D., & Zimmermann, F. K. (1982). Genetic analysis of the pyruvate decarboxylase reaction in yeast glycolysis. *Journal of Bacteriology*, *151*(3), 1146–1152.

Seaman, M. N., McCaffery, J. M., & Emr, S. D. (1998). A membrane coat complex essential for endosome-to-Golgi retrograde transport in yeast. *The Journal of Cell Biology*, *142*(3), 665–681.

Semple, J. I., Vavouri, T., & Lehner, B. (2008). A simple principle concerning the robustness of protein complex activity to changes in gene expression. *BMC Systems Biology*, *2*, 1.

Sentenac, A. (1985). Eukaryotic RNA polymerases. *CRC Critical Reviews in Biochemistry*, *18*(1), 31–90.

Sopko, R., Huang, D., Preston, N., Chua, G., Papp, B., Kafadar, K., Snyder, M., Oliver, S. G., Cyert, M., Hughes, T. R., Boone, C., & Andrews, B. (2006). Mapping pathways and phenotypes by systematic gene overexpression. *Molecular Cell*, *21*(3), 319–330.

Stingele, S., Stoehr, G., Peplowska, K., Cox, J., Mann, M., & Storchova, Z. (2012). Global analysis of genome, transcriptome and proteome reveals the response to aneuploidy in human cells. *Molecular Systems Biology*, *8*, 608.

Taggart, J. C., & Li, G.-W. (2018). Production of Protein-Complex Components Is Stoichiometric and Lacks General Feedback Regulation in Eukaryotes. In *Cell Systems* (Vol. 7, Issue 6, pp. 580–589.e4). https://doi.org/10.1016/j.cels.2018.11.003

Taggart, J. C., Zauber, H., Selbach, M., Li, G.-W., & McShane, E. (2020). Keeping the Proportions of Protein Complex Components in Check. *Cell Systems*, *10*(2), 125–132.

Tanaka, J., & Fink, G. R. (1985). The histidine permease gene (HIP1) of Saccharomyces cerevisiae. *Gene*, *38*(1-3), 205–214.

Tanaka, K., Matsumoto, K., & Toh-E, A. (1989). IRA1, an inhibitory regulator of the RAS-cyclic AMP pathway in Saccharomyces cerevisiae. *Molecular and Cellular Biology*, *9*(2), 757–768.

Tarassov, K., Messier, V., Landry, C. R., Radinovic, S., Serna Molina, M. M., Shames, I., Malitskaya, Y., Vogel, J., Bussey, H., & Michnick, S. W. (2008). An in vivo map of the yeast protein interactome. *Science*, *320*(5882), 1465–1470.

Tong, A. H. Y., & Boone, C. (2006). Synthetic genetic array analysis in Saccharomyces cerevisiae. *Methods in Molecular Biology* , *313*, 171–192.

Torres, E. M., Dephoure, N., Panneerselvam, A., Tucker, C. M., Whittaker, C. A., Gygi, S. P., Dunham, M. J., & Amon, A. (2010). Identification of aneuploidy-tolerating mutations. *Cell*, *143*(1), 71–83.

Velmurugan, S., Lobo, Z., & Maitra, P. K. (1997). Suppression of pdc2 regulating pyruvate decarboxylase synthesis in yeast. *Genetics*, *145*(3), 587–594.

Wang, M., Weiss, M., Simonovic, M., Haertinger, G., Schrimpf, S. P., Hengartner, M. O., & von Mering, C. (2012). PaxDb, a database of protein abundance averages across all three domains of life. *Molecular & Cellular Proteomics: MCP*, *11*(8), 492–500.

Velmurugan, S., Z. Lobo, and P. K. Maitra. 1997. “Suppression of pdc2 Regulating Pyruvate Decarboxylase Synthesis in Yeast.” *Genetics* 145 (3): 587–94.

Supplementary Information

Supplementary Figures

Figure S1. Results from the competition experiment in ionic and osmotic stress.
Figure S2. Selection coefficients of strains carrying extra copies of subunits of complexes.
Figure S3. Heatmaps of wild-type interactions for the Retromer, the Proteasome, and the RNA polymerases I, II, and III.
Figure S4. Normalized GFP signals of all tested GFP-fusions of proteasome subunits in a wild-type background.
Figure S5. Correlation between protein-abundance change after duplication of proteasome subunits with the protein-abundance data reported from PaxDb.
Figure S6. Pre7p attenuation is dosage-dependent
Figure S7. Expression changes of genes with interactions not perturbed by the duplication of PRE7.
Figure S8. The response of the proteasome to disomic chromosomes encoding its subunits.
Figure S9. Duplicated *PRE7* copies mutagenized with premature stop codons are not attenuated.

Supplementary Tables

Table S1. Selection coefficients in fluorometry in SD and in 1.2M NaCl.
Table S2. Selection coefficients of competition assays performed in cytometry.
Table S3. Sensitivity to different z-score thresholds.
Table S4. List of preys, baits, and plasmids used for the PCA experiments.
Table S5. DHFR-PCA data: colony sizes, *q-values*, and *ps*.
Table S6. Cytometry GFP measurements and attenuation scores.
Table S7. Cytometry GFP data of the tunable promoter system experiments with PRE7.
Table S8. Cytometry data for duplication of PRE7 in all the other subunits GFP-fusion strains.
Table S9. Oligonucleotides used in this study (confirmations, GFP-tagging, plasmid construction).
Table S10. Media and solutions used in this study.

Supplementary Figure S1

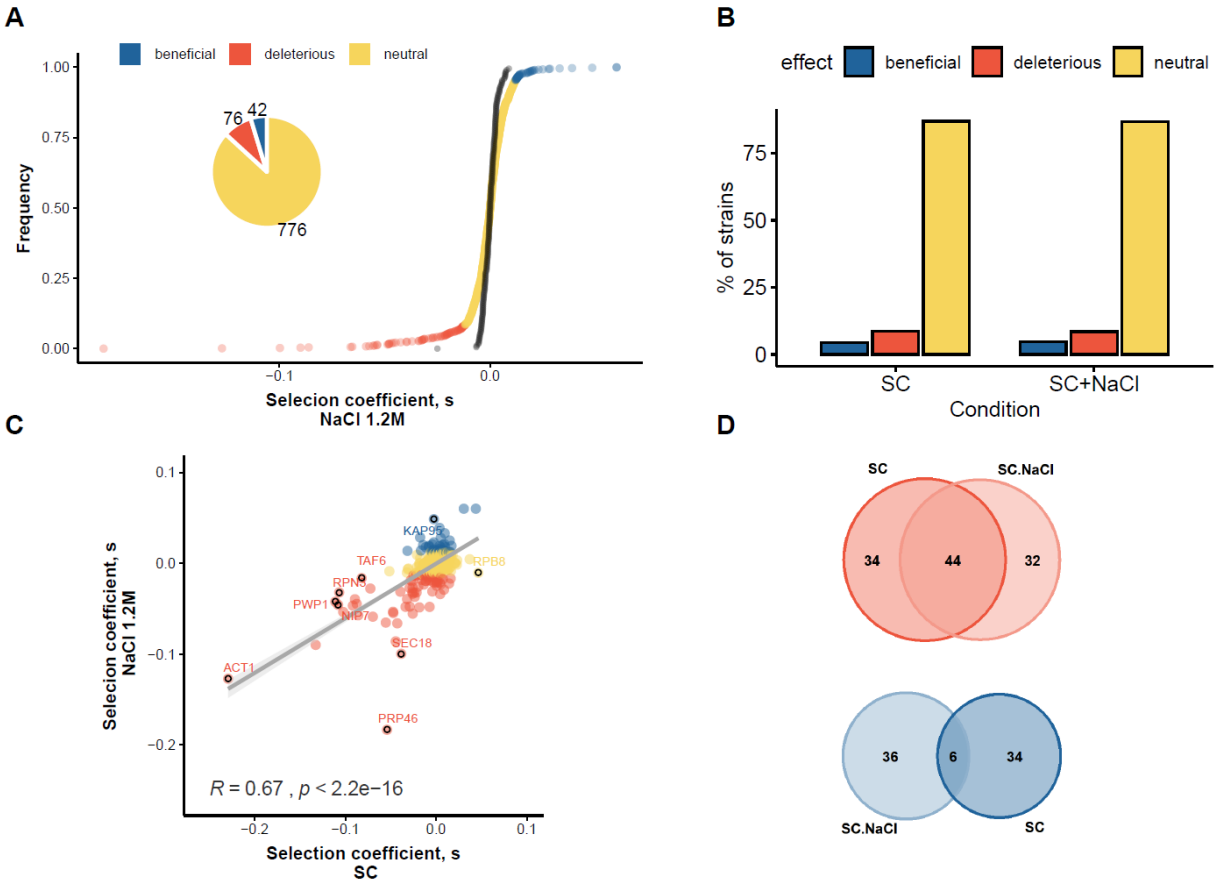

Figure S1. Results from the competition experiment in ionic and osmotic stress. (**A**) Cumulative distribution of the selection coefficients of strains with additional copies of essential genes tested in stress. Experimental conditions are the same as the nominal media. Genes are classified in neutral, deleterious and beneficial using (selection coefficient > 0.01 or < -0.01, |z-score| > 4.5). (**B**) Percentage of strains that are neutral (yellow bars), deleterious (red bars), and beneficial (blue bars) effects in both conditions tested. (**C**) Comparison of selection coefficients in both conditions. Pearson's correlation coefficient and p-value are shown on the bottom. Black circles highlight strains within more than a 5% difference in relative fitness between the two conditions. (**D**) Venn diagrams for genes with fitness effects in both conditions.

Supplementary Figure S2

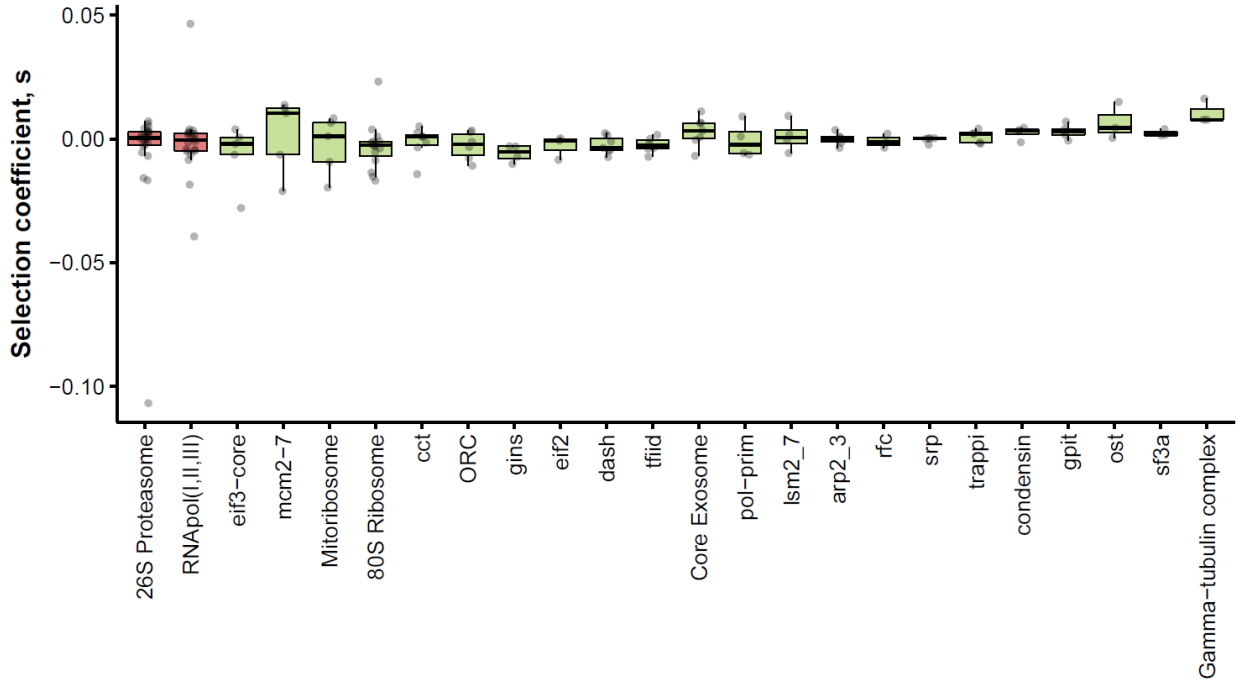

Figure S2. Selection coefficients of strains carrying extra copies of subunits of complexes. The list of proteins that are members of protein complexes was obtained from the Complex Portal Database (https://www.ebi.ac.uk/complexportal/home). Complexes are ordered according to their most deleterious duplication. In red we show the complexes selected for further experiments.

Supplementary Figure S3

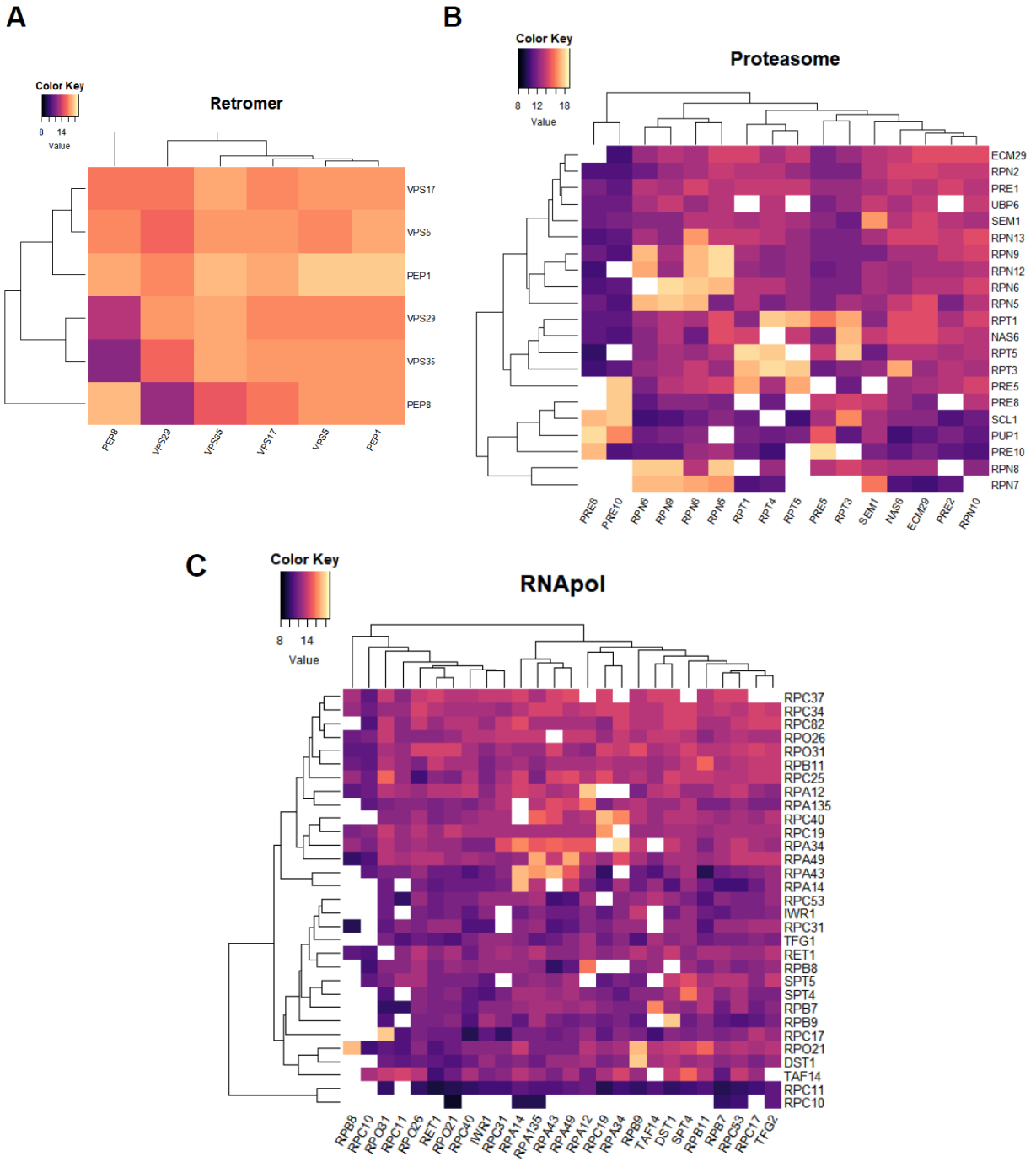

Figure S3. Heatmaps of wild-type interactions of the (**A**) retromer complex; (**B**) 26S Proteasome Complex and (**C**) RNA polymerase I, II, and III. Each tile represents a different diploid strain obtained from the mating of the preys strains (MATα prey-DHFR-F[3]) indicated in the columns and the baits (MATa bait-DHFR-F[1,2]) indicated in the rows. The values on the color key represent the size of the colony of that diploid strain at the fourth day of the MTX II selection plate. White tiles represent missing values. Colony sizes above 14.7 are considered positive interactions (see methods).

Supplementary Figure S4

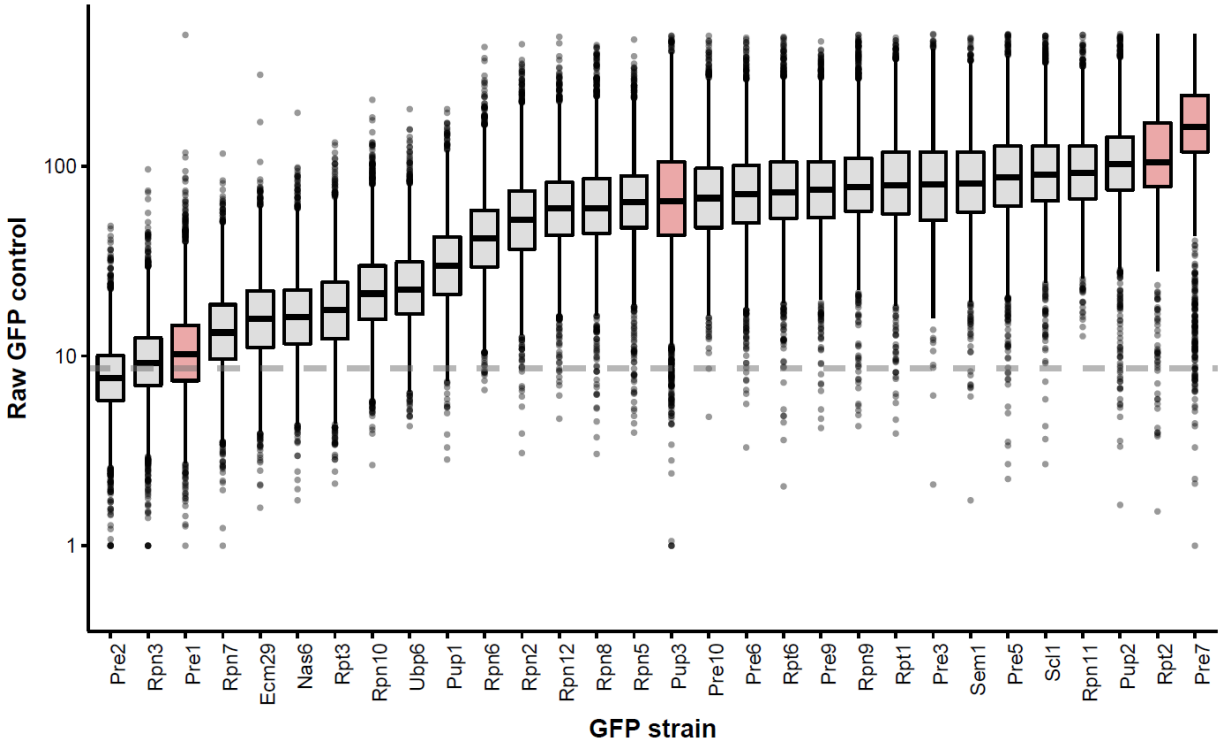

Figure S4. Raw GFP signals of all tested GFP-fusions of proteasome subunits in a wild-type background. In gray, strains obtained from the Yeast GFP Fusion Collection (Huh et al. 2003). In red, strains generated in this work. For further analyses, raw GFP values were normalized using the autofluorescence signal of the parental strain BY4741 not expressing GFP. The median of this strain is represented by a dashed line.

Supplementary Figure S5

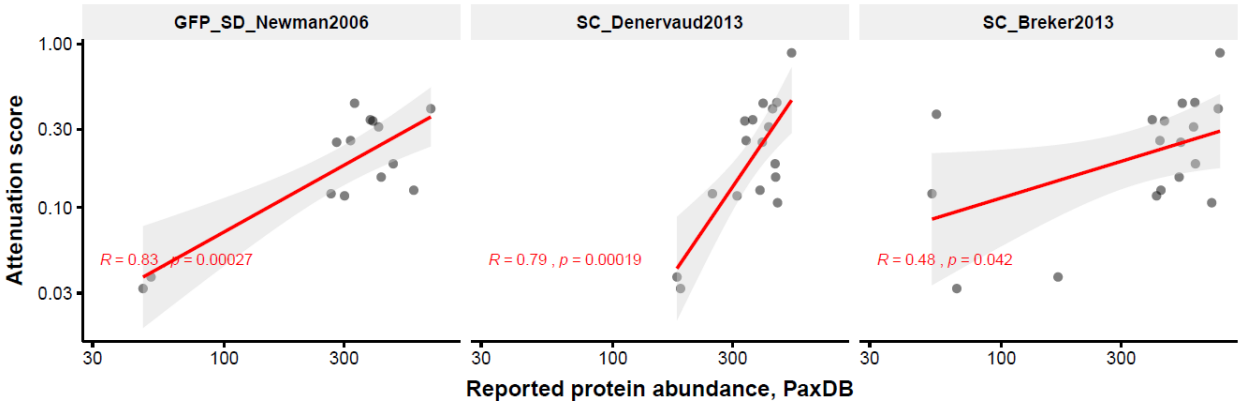

Figure S5. Correlation between attenuation and the protein abundance reported in other studies. Data were retrieved from PaxDb (Wang et al., 2012). On bottom, we present Pearson's correlation coefficients and *p-values*.

Supplementary Figure S6

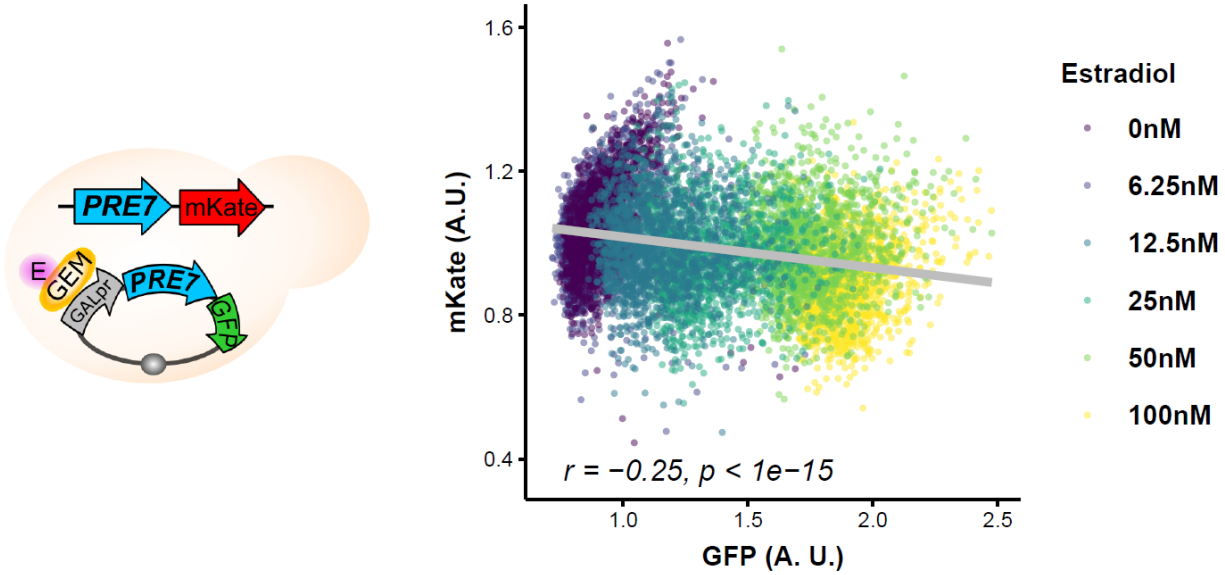

Figure S6. Pre7p attenuation is dosage dependent. On the left, a cartoon of the strain used for this experiment. The genomic copy of *PRE7* is tagged with mKate. The strain was transformed with a plasmid bearing an extra copy of *PRE7* expressed under the *GAL1* promoter and tagged with GFP. The parental strain that expresses the GEM (yellow oval) chimeric transcriptional regulator (Aranda-Díaz et al., 2017) is activated in the presence of estradiol (pink circle). On the right, the mKate fluorescent signal (*PRE7* chromosome-coded copy) as a function of the GFP signal (plasmid-coded copy). Each point represents an event detected by flow cytometry. We captured up to 5,000 events for each concentration of estradiol. Colors represent different estradiol concentrations (*Supplementary TableS8*).

Supplementary Figure S7

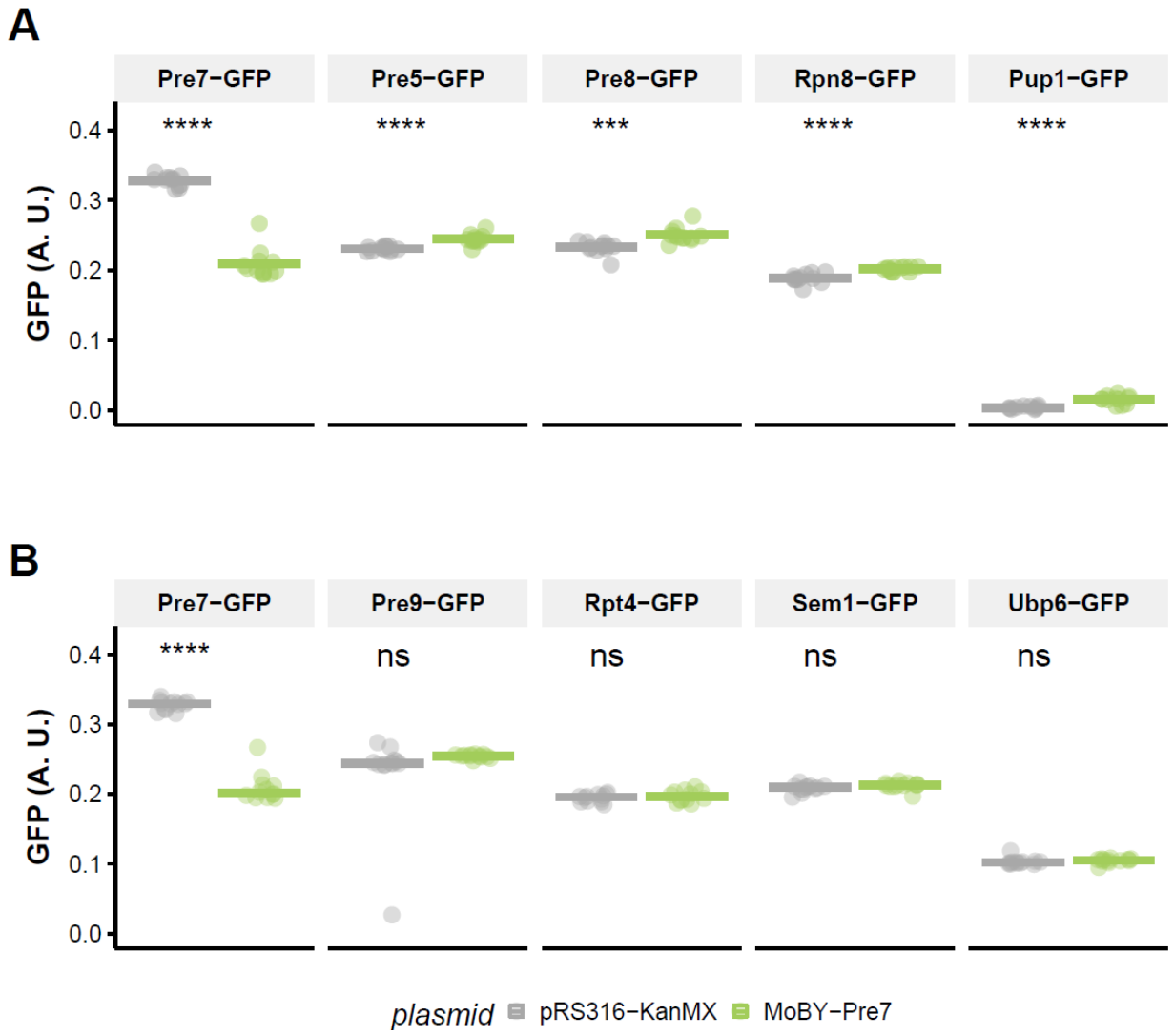

Figure S7. Abundance changes of various proteins in the genetic background of PRE7 duplication. Average GFP signal of proteasome subunits with PPIs (**A**) perturbed and (**B**) non-perturbed by PRE7 duplication. In green, GFP-strains carrying *PRE7* duplication and, in gray, strains carrying the empty vector as a control. Each dot represents a biological replica and is the mean of up to 5,000 events measured by flow cytometry. The horizontal bar indicates the median of the 12 biological replicas. The GFP signals are normalized with the autofluorescence signal of the parental strain BY4741 not expressing GFP. Each strain was isolated from an independent colony of the transformation plates. On top, we show the *p*-values of Student's T-test (***: $p < 0.001$; ****: $p < 0.0001$; ns: $p > 0.05$).

Supplementary Figure S8

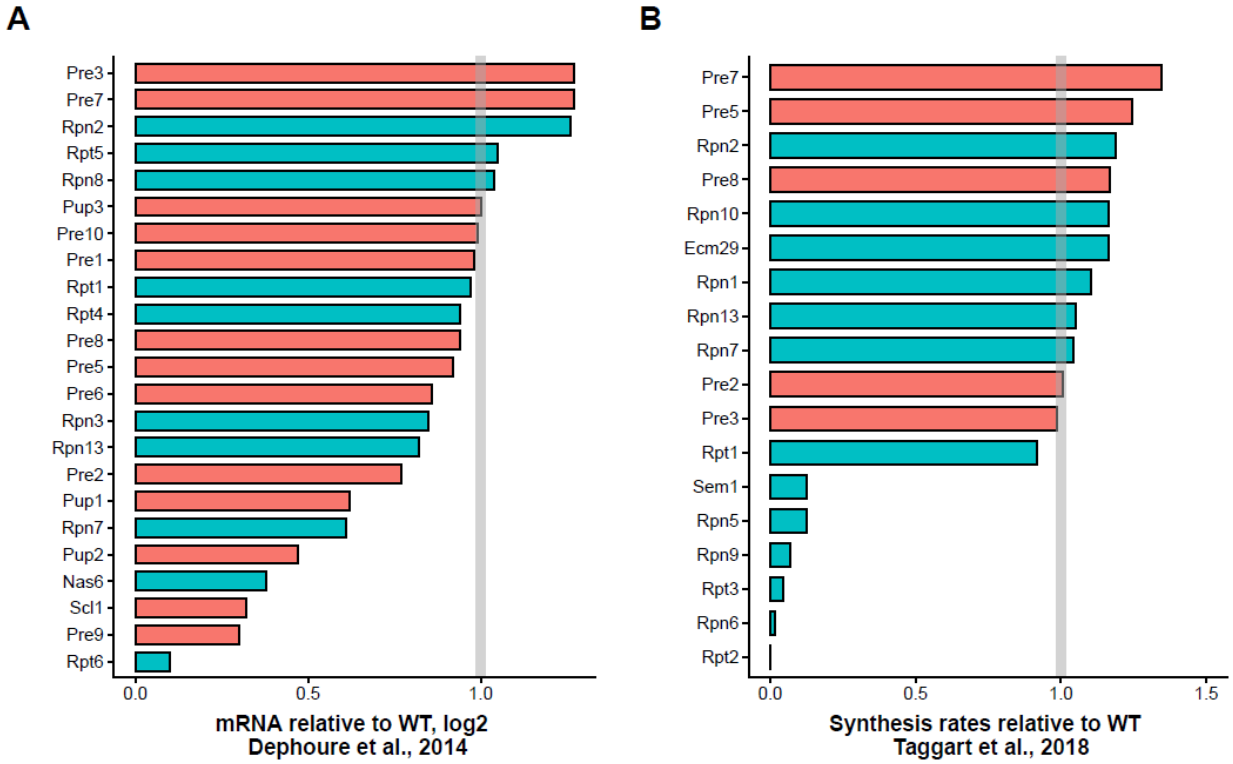

Figure S8. The response of the proteasome to disomic chromosomes encoding its subunits. Change in (**A**) mRNA abundance and in (**B**) synthesis rates estimated by ribosome profiling of duplicated proteasome subunits relative to wild-type (single-copy). mRNA data was obtained from Dephoure *et al*. (2014). In this genome-wide screening, they estimate the mRNA abundance of individual genes in aneuploid strains relative to a wild-type. Synthesis rate data obtained from Taggart *et al*. (2018) and derived from ribosome profiling. The gray line represents the expected value when there is no feedback regulation after the duplication of these subunits.

Supplementary Figure S9

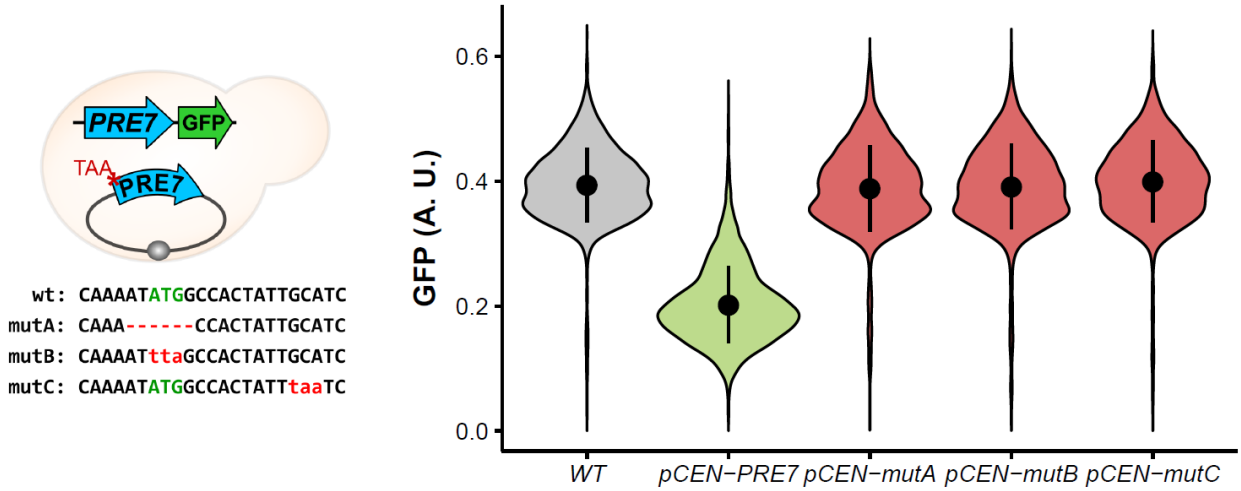

Figure S9. Duplicated *PRE7* copies mutagenized with premature stop codons are not attenuated. On the left, we show a cartoon of the strain bearing a mutagenized *pCEN-PRE7* plasmid and the GFP-tagged *PRE7* genomic copy. In the plasmid *pCEN-mutA*, we deleted the start codon of *PRE7*, on the *pCEN-mutB* plasmid, we replaced the start codon with a stop codon, and in the *pCEN-mutC* plasmid, we replaced the fifth codon with a stop codon. All strains are constructed in the *PRE7-GFP* background (see Methods). On the right, each violin-plot shows the distribution of 5,000 cells GFP normalized signal measured by flow cytometry.